

CHAPTER 5

Propionibacterium acnes and *Helicobacter pylori* lipases: isolation, characterization and inhibition by natural substances

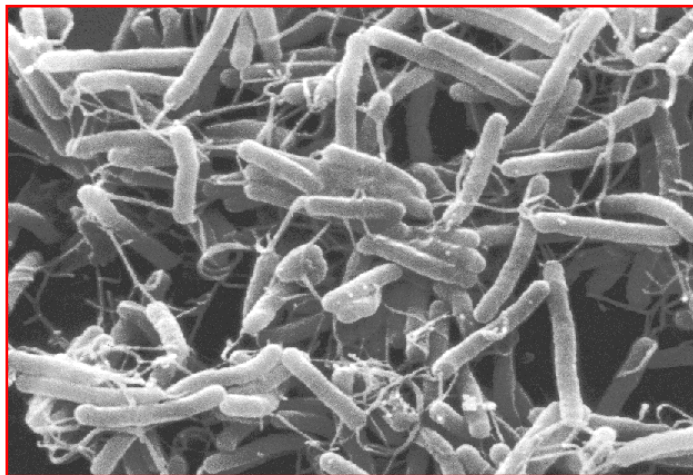


Figure C5.1 *H. pylori* cells (<http://www.helico.com>).

1 INTRODUCTION AND OBJECTIVES

Several lipases produced by microbial pathogens play an important role in infective diseases, being *P. acnes* lipase (GehA) and *H. pylori* lipase(s) among the most the most interesting from a clinical point of view (General Introduction 3.4).

P. acnes lipase and its inhibition by anti-acne compounds have been studied because the fatty acids produced by GehA activity on sebaceous triglycerides induce severe inflammation, and are involved in the plugging of the sebaceous follicle ducts and in biofilm formation (Higaki, 2003; General Introduction 3.4.1). For this reason, several efforts have been performed for the isolation, characterization and inhibition of this lipase, including its cloning and expression in *E. coli* by Miskin *et al.* (1997).

In addition, *H. pylori* lipase activity, which is inhibited by some antiulcer drugs, can weaken the barrier properties of mucus by hydrolyzing endogenous lipids, and seems to be related to the disruption of epithelial cells and to the generation of cytotoxic and pro-inflammatory lipids (Tsang & Lam, 1999; General Introduction 3.4.2). For this reason, several studies on the inhibition of *H. pylori* lipase by antiulcer agents have been performed (Slomiany *et al.*, 1989a, 1989b, 1992a and 1992b; Piotrowski *et al.*, 1991 and 1994; Otlecz *et al.*, 1999). However, the number and biochemical properties of the lipase(s) produced by this bacterium remain almost unknown, since only related enzymes such as *H. pylori* phospholipases A₂ and C have been cloned and/or characterized (Weitkamp *et al.*, 1993; Dorrell *et al.*, 1999; General Introduction 3.4.2).

Therefore, this chapter is focused on the isolation and characterization of lipases from these two pathogenic strains, in order to increase our knowledge about their biochemical properties, as well as on the inhibition of these lipases by natural substances that could be useful for the prevention and therapy of acne, peptic ulcer and other diseases produced by *P. acnes* and *H. pylori*. The exact aims of this work were:

1. To clone and characterize the lipase GehA of *Propionibacterium acnes* P-37.

- a. To clone and express the gene *gehA* of *Propionibacterium acnes* P-37 in *Escherichia coli* XL1-Blue.
- b. To perform the molecular and biochemical characterization of the lipase GehA of *P. acnes* P-37 in order to confirm and increase the knowledge about the biochemical features of this enzyme.

2. To isolate, clone and characterize the lipase(s) of *Helicobacter pylori* 26695.

- c. To analyze the genome and putative proteome of *Helicobacter pylori* 26695 in order to select those putative ORFs showing similarity to previously described bacterial lipases.
- d. To clone and express in *Escherichia coli* DH5 α the gene *HP0739* of *H. pylori* 26695, which was selected during the analysis of the genome of this strain as the best lipase-coding gene candidate, and to confirm the lipolytic activity of the encoded protein HP0739 (EstV).
- e. To perform the purification of the enzyme HP0739 (EstV).
- f. To perform the molecular and biochemical characterization of HP0739 (EstV).

3. To evaluate the effect of the most potent lipase inhibitors found in Chapter 4 on *Propionibacterium acnes* GehA and *Helicobacter pylori* HP0739 (EstV).

- g. Saponins: β -aescin, digitonin, glycyrrhizic acid and *Quillaja* saponin.
- h. Flavonoids: (\pm)-catechin and kaempferol.
- i. Alkaloids: rescinnamine and reserpine.

◆ **NOTE:** The work presented in this chapter was performed in collaboration with Dr. S. Falcocchio from the Università degli studi di Roma “*La Sapienza*”.

2 MATERIALS AND METHODS

Unless otherwise stated, the materials and methods used were those previously described in the General Materials and Methods section (see Tables M.1, M.2, M.3 and M.7 for a more detailed explanation of the strains, culture media, plasmids and primers used).

2.1 CLONING AND EXPRESION OF *P. acnes* P-37 *gehA*

2.1.1 Cloning of *P. acnes* P-37 *gehA*

Strain *P. acnes* P-37, kindly provided by Dr. M.D. Farrar and Dr. K.T. Holland, was cultured on Reinforced Clostridial Agar under anaerobic conditions as previously described (General Materials and Methods Table M.1). The resulting colonies were suspended in distilled water and used as template for PCR amplifications using the primers PALIPFW and PALIPBW, designed for the specific isolation of *P. acnes gehA*, including the upstream (76 bp) and downstream (84 bp) regions of this gene, and bearing the sequence for the restriction nucleases *XbaI* and *PstI*, respectively. Amplification by PCR was performed using *Pfu* polymerase and a Tm of 50 °C, and the resulting amplified fragment was purified and sequenced in order to confirm its nucleotide sequence. The amplified DNA fragment was then digested using the restriction enzymes *XbaI* and *PstI*, and subsequently ligated to *XbaI*–*PstI*-digested pUC19 plasmid. The resulting recombinant plasmid pUC-GehA was transformed into *E. coli* XL1-Blue to obtain the recombinant clone *E. coli* XL1-Blue–pUC-GehA, which was selected on the basis of its ampicillin resistance and white color on LB-Ap-Tc plates supplemented with IPTG and X-gal. The sequence of the insert was then re-confirmed, and studied by computational analysis (General Material and Methods 3.7).

The lipolytic activity of the recombinant clone obtained was screened on lipid-supplemented CeNAN agar plates and by the classical fluorimetric liquid assay, using crude cell extracts from this clone and MUF-derivative substrates (General Materials and Methods 5.1.1 and 5.4.2.1, respectively). Crude cell extracts (50-fold concentrated) were prepared in 50 mM phosphate buffer (pH 7) as previously described in General Materials and Methods 4.1.1

2.1.2 Production of GehA in *E. coli*

Crude cell extracts of the recombinant clone *E. coli* XL1-Blue-pUC-GehA were used for production of the GehA protein used in the molecular and biochemical characterization of this enzyme, and in the inhibition assays by natural substances. Although this clone was active on lipid-supplemented plates (containing also IPTG), did not show activity on liquid assays due to the formation of inactive and insoluble aggregates of GehA when it is expressed in *E. coli* (Miskin *et al.*, 1997). Thus, obtaining active cell extracts required the preparation of *E. coli* XL1-Blue-pUC-GehA cultures on LB-Ap medium supplemented with 0.45 M saccharose, and the incubation of these cultures at 25 °C. When the $A_{600\text{ nm}}$ was 0.6–1, 1 mM IPTG was added, and the culture was incubated for 2 h before preparing 50-fold concentrated cell extracts in 50 mM phosphate buffer (pH 7).

2.2 ISOLATION, CLONING AND PURIFICATION OF A NOVEL LIPOLYTIC ENZYME OF *H. pylori* 26695

2.2.1 Analysis of *H. pylori* 26695 genome and selection of a lipase-coding gene candidate

The knowledge of the genome sequence of *H. pylori* 26695 (Tomb *et al.*, 1997) allowed us to perform a screening of the putative proteins of this strain in order to detect

those ORFs with the highest similarity to known lipases. For this purpose, the amino acid sequence of the lipases used by Arpigny and Jaeger (1999) and by Jaeger and Eggert (2002) to elaborate the classification of bacterial lipases (see General Introduction Table I.5), as well as the sequence of some eukaryotic lipases such as *Candida albicans* Lip8 (AF191321), *Canis familiaris* gastric lipase (P80035), human gastric lipase precursor (P07098), human pancreatic lipase (P54315) and human precursor of lipoprotein lipase (P06858), were analyzed through BLAST search against the putative proteins of *H. pylori* 26695 (Tomb *et al.*, 1997) as previously described (General Materials and Methods 3.7).

Those ORFs showing the highest similarity, or being similar to a major number of known lipases, were chosen and re-analyzed through BLAST search against all kind of enzymes in order to select those showing a higher similarity to known lipases than to other enzymes. The higher similarity to lipases than to other enzymes of the candidates selected was confirmed by using ClustalW Multalign on-line software (General Materials and Methods 3.7).

The candidates selected during the previous steps were then analyzed for the detection of the general protein motifs of lipases (α/β hydrolase fold, the Ser-Asp/Glu-His catalytic triad, the conserved Gly/Ala-Xaa-Ser-Xaa-Gly pentapeptide, etc), and for the detection of the conserved motifs of the lipase family to which they showed the highest similarity. From these results, the putative protein HP0739, which was named EstV due to its similarity to the carboxylesterases from family V of bacterial lipases (Arpigny & Jaeger, 1999), was considered as the best lipase candidate. Thus, the molecular properties and structural arrangements of this putative protein were studied by computational analysis as previously described (General Materials and Methods 3.7).

2.2.2 Cloning of *H. pylori* 26695 *estV* and confirmation of the lipolytic activity of EstV

Strain *H. pylori* 26695, cultured on Columbia agar supplemented with 5% lysed defibrinated horse blood for 4 days and under microaerophilic conditions, was kindly

provided by N. Queralto and Dr. R. Araujo. Several colonies from these cultures were suspended in distilled water and used as template for PCR amplifications using the primers HP0739FW and HP0739BW, designed for the specific amplification of *estV* (including the upstream – 132 bp – and downstream – 166 bp – regions), and bearing the sequence for the restriction nucleases *XbaI* and *PstI*, respectively. Amplification by PCR was performed using *Pfu* polymerase and a T_m of 43 °C, and the resulting fragment was purified, sequenced, digested using the restriction enzymes *XbaI* and *PstI*, ligated to *XbaI*–*PstI*-digested pUC19 plasmid, and transformed into *E. coli* XL1-Blue and *E. coli* DH5 α . However, no recombinant clones could be obtained. No results were either obtained by blunt-end ligation of the PCR band to *SmaI*-digested pUC19 plasmid followed by transformation into both *E. coli* strains. For this reason, the process was repeated using the primers HPESTFW and HPESTBW, designed for the specific amplification of *estV* ORF and a few nucleotides of the upstream (11 bp, containing the ribosome binding site) and downstream (15 bp) regions of this gene. These primers contained the sequence for the restriction nucleases *NdeI* and *BamHI*, respectively. Amplification by PCR was performed using *Pfu* polymerase and a T_m of 48 °C, and the resulting DNA fragment was purified and sequenced in order to confirm its nucleotide sequence. After that, the amplified fragment was ligated (blunt-end ligation) to *SmaI*-digested pUC19 plasmid, and the resulting recombinant plasmid pUC-EstV was transformed into *E. coli* DH5 α to obtain the recombinant clone *E. coli* DH5 α -pUC-EstV, which was selected on the basis of its ampicillin resistance and white color on LB-Ap plates containing IPTG and X-gal. The nucleotide sequence of the insert of this clone was also determined for its confirmation.

The lipolytic activity of *E. coli* DH5 α -pUC-EstV was detected on lipid-supplemented CeNAN agar plates, and was determined by classical fluorimetric liquid assay using MUF-derivative substrates and crude cell extracts from this clone prepared in 50 mM phosphate buffer (pH 7). These cell extracts were also used to perform EstV purification assays by FPLC (Fast Protein Liquid Chromatography).

A second cloning process of *HP0739* was performed by *NdeI*–*BamHI*-digestion of the plasmid pUC-EstV, followed by re-isolation of the digested insert, and ligation to the *NdeI*–*BamHI*-digested pET28a plasmid. The resulting recombinant pET28a-EstV plasmid, showing the following configuration: T7 promoter/*lac* operator/N-terminal 6-

His tag/thrombin cleavage site/HP0739/T7 terminator (see General Materials and Methods 4.3.1.1), was transformed first into *E. coli* DH5 α and then into *E. coli* BL21(DE3) to obtain the recombinant clone *E. coli* BL21(DE3)–pET28-EstV used for EstV purification by the His-tag system (Novagen).

2.2.3 Purification of *H. pylori* EstV

Purification of protein EstV was first performed through the His-tag system as previously described (General Materials and Methods 4.3.1). Briefly, the clone *E. coli* BL21(DE3)–pET28-EstV was cultured on LB Kan at 37 °C. When the $A_{600\text{ nm}}$ was 0.5–0.6, 1 mM IPTG was added and the culture was incubated for 3 h before preparing the corresponding cell extract in lysis buffer. Purification of His-EstV from the cell extract was carried out by affinity chromatography using NTA-Ni resin, and the purified proteins were recovered and analyzed by SDS-PAGE and zymogram analysis before removing its His-tail. However, no properly purified protein was obtained by this system.

For this reason, EstV purification was also attempted by using the FPLC system as described before (General Materials and Methods 4.3.2). Briefly, *E. coli* DH5 α –pUC-EstV was grown on LB-Ap at 37 °C and when the $A_{600\text{ nm}}$ was 0.5–0.6, 1 mM IPTG was added. The culture was then incubated overnight before preparing the cell extract in 50 mM phosphate buffer (pH 7), which was subsequently treated with streptomycin sulphate and ammonium sulphate. The precipitated proteins were then suspended in 50 mM phosphate buffer (pH 7), and separated in an AKTA FPLC chromatographic system by four steps: gel filtration (by size), ion exchange (by charge), gel filtration and ion exchange. Lipase-containing fractions were detected by colorimetric microassay (General Materials and Methods 5.3.2), and were analyzed by SDS-PAGE and zymogram. Those fractions containing the purified lipase EstV were used for N-terminal sequencing of the protein, for the biochemical and molecular characterization of the enzyme, and for inhibition assays by natural substances.

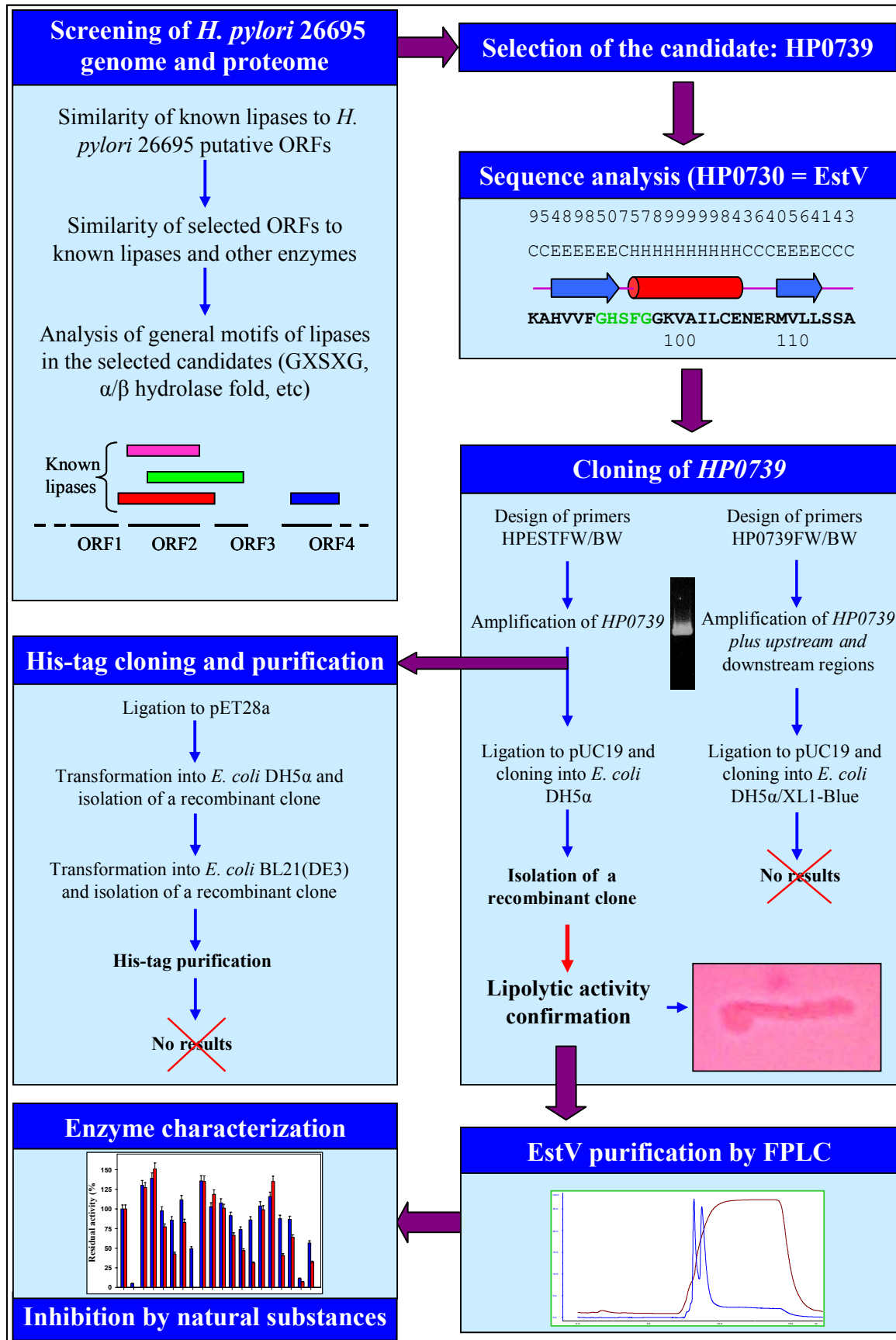


Figure C5.2 Isolation, cloning and purification of *H. pylori* 26695 EstV.

2.3 CHARACTERIZATION AND INHIBITION OF GehA AND EstV

Crude cell extracts from *E. coli* XL1-Blue-pUC-GehA clone prepared as described before (cultures on LB supplemented with saccharose and incubated at 25 °C) and purified fractions of EstV were used for the molecular and biochemical characterization of *P. acnes* P-37 GehA and *H. pylori* 26695 EstV, as well as to analyze their inhibition by natural substances. To take into account the background activity of the 50-fold concentrated cell extracts, the activity of GehA-containing cell extracts other than that produced by GehA was subtracted by using the activity values of *E. coli* XL1-Blue-pUC19 cell extracts prepared and assayed under the same conditions as the cell extracts from *E. coli* XL1-Blue-pUC-GehA.

2.3.1 Biochemical and molecular characterization of GehA and EstV

Molecular characterization was performed by zymogram analysis after SDS-PAGE or Native-PAGE gels (General Materials and Methods 5.2, 4.1.1 and 4.1.2, respectively). Biochemical characterization was performed as described (General Materials and Methods 5.6), using the classical and the new fluorimetric liquid assays (General Materials and Methods 5.4.2.1 and 5.4.2.2, respectively) to determine the optimum temperature and the optimum pH of the cloned enzymes, and the enzyme kinetics of EstV, and using the colorimetric microassay (General Materials and Methods 5.3.2 and Chapter 3), performed at pH 7 and at the optimum temperature of the cloned enzymes at this pH, to determine the substrate range and specificity of these lipases, and to determine the enzyme kinetics of GehA.

Inhibition-activation assays in the presence of 1 mM and 10 mM cations, amino acid modifying agents and other agents were performed by colorimetric microassay using *p*-NP laurate (*p*-NPL) as substrate, as previously described (General Materials and Methods 5.7). The assays were performed at pH 7 and at the optimum temperature of the cloned enzymes at this pH.

Biochemical characterization experiments and inhibition–activation assays were performed in triplicate, being each replicate the result of an independent assay performed in duplicate.

2.3.2 Effect of natural substances on GehA and EstV

Inhibition assays in the presence of saponins (β -aescin, digitonin, glycyrrhizic acid and *Quillaja* saponin), flavonoids ((\pm)-catechin and kaempferol) and alkaloids (rescinnamine and reserpine) were performed at 37 °C and pH 7 through the colorimetric microassay and using *p*-NP laurate (*p*-NPL) as substrate (General Materials and Methods 5.7 and Chapter 4). These experiments were performed in triplicate, being each replicate the result of an independent assay performed in duplicate, and the concentrations yielding a lipase inhibition of 16% (IC₁₆) and 50% (IC₅₀) were calculated by regression analysis with Rsquare coefficients higher than 0.99, as previously described (General Materials and Methods 5.7).

3 RESULTS

3.1 CLONING AND CHARACTERIZATION OF *P. acnes* P-37 GehA

3.1.1 Cloning and analysis of GehA

Strain *P. acnes* P-37 was used for PCR amplification of the gene *gehA*, encoding for *P. acnes* lipase (GehA), as is described in the Materials and Methods. A DNA fragment of ca. 1.2 kb was obtained, ligated into pUC19 and transformed into *E. coli* XL1-Blue to obtain the recombinant clone *E. coli* XL1-Blue-pUC-GehA.

The nucleotide sequence of the cloned DNA was determined, confirming that it was identical to the *gehA* sequence (X99255) reported by Miskin *et al.* (1997). This gene contained an ORF of 1017 nucleotides encoding for GehA, as well as the upstream (76 bp) and downstream (84 bp) regions of this gene, including part of the promoter and the transcription terminator of the gene.

Analysis of the predicted GehA protein confirmed that it was a protein of 339 amino acids with a MW of 35995 Da with a N-terminal signal peptide of 26 residues whose cleavage yielded a mature protein of 313 residues and 33396 Da, as previously described by Miskin *et al.* (1997). Moreover, theoretical pIs of 6.59 and 6.26 for the non-mature and mature forms of this protein were determined. GehA showed also a high content in short non-polar residues (42% of the total; Table C5.1) as is usual in enzymes acting on hydrophobic substrates that can be found in aggregated state (Fojan *et al.*, 2000).

GehA showed the highest identity (50%) to *Streptomyces cinnamoneus* lipase (Sommer *et al.*, 1997), the other member of subfamily I.7 of bacterial lipases (Jaeger & Eggert, 2002), whereas its identity to other lipases from family I of bacterial lipases was lower. As described before (Miskin *et al.*, 1997), amino acid sequence alignments confirmed that the catalytic serine was located at position 169 of the non-processed

protein, included in the pentapeptide Gly-His-Ser-Gln-Gly that corresponds to the conserved Gly-Xaa-Ser-Xaa-Gly pentapeptide of lipases (Fojan *et al.*, 2000).

Table C5.1 Amino acid composition of GehA.

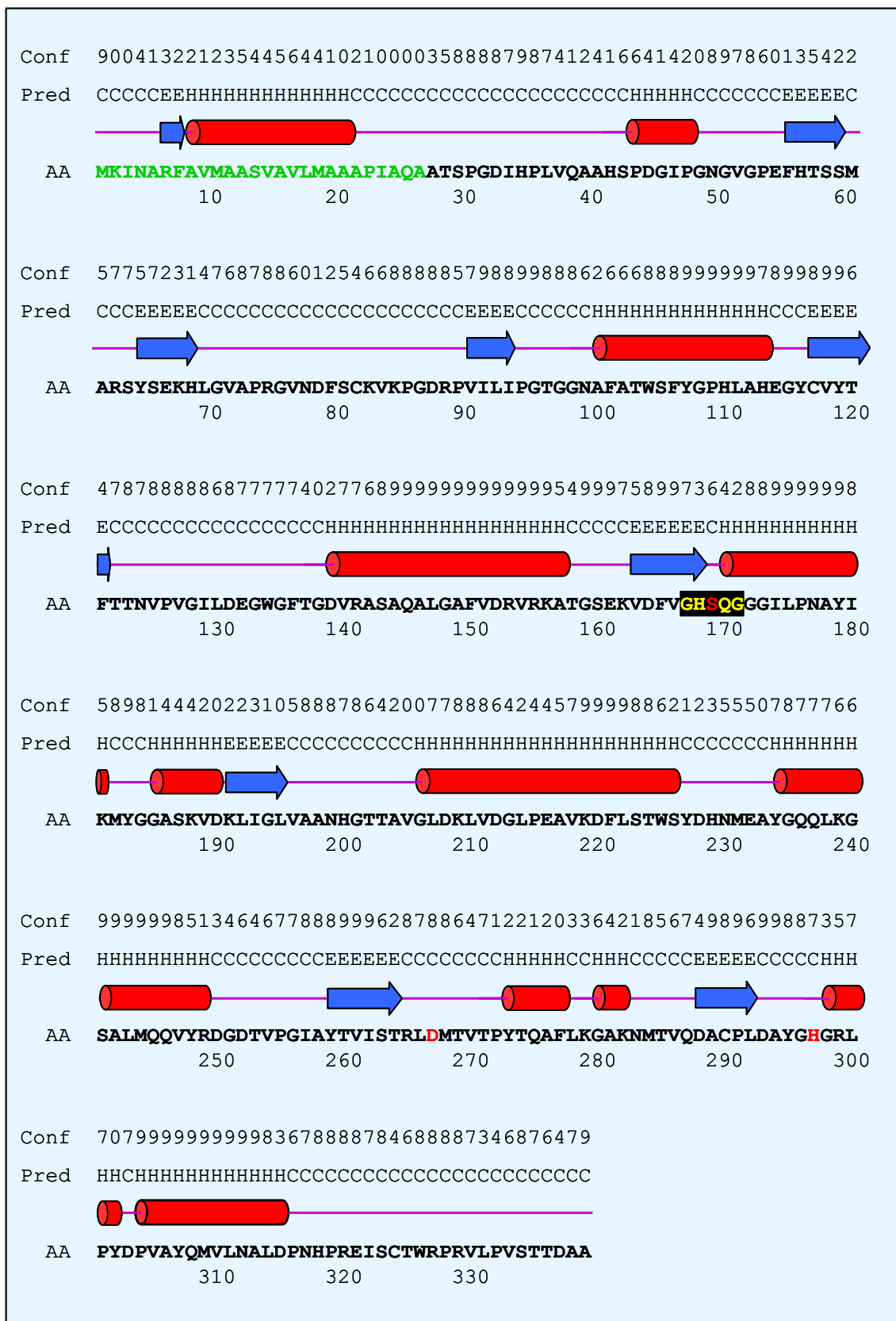
Ala (A)	40	11.8%	Gly (G)	36	10.6%	Pro (P)	23	6.8%
Arg (R)	13	3.8%	His (H)	11	3.2%	Ser (S)	19	5.6%
Asn (N)	11	3.2%	Ile (I)	13	3.8%	Thr (T)	22	6.5%
Asp (D)	21	6.2%	Leu (L)	23	6.8%	Trp (W)	4	1.2%
Cys (C)	4	1.2%	Lys (K)	14	4.1%	Tyr (Y)	14	4.1%
Gln (Q)	11	3.2%	Met (M)	10	2.9%	Val (V)	31	9.1%
Glu (E)	8	2.4%	Phe (F)	11	3.2%			

- Total number of negatively charged residues (Asp + Glu): **29**
- Total number of positively charged residues (Arg + Lys): **27**
- Short non-polar residues (Ala + Gly + Ileu + Leu + Val) = **143 (42.5%)** □

A three-dimensional model of this enzyme could not be obtained since it showed low similarity to lipases of known structure. Nevertheless, protein fold recognition using 1D and 3D sequence profiles coupled with secondary structure information allowed us to predict that GehA was a globular, compact protein with a single domain, belonging to the group of serine-hydrolases and displaying the typical α/β hydrolase fold of lipases (Jaeger *et al.*, 1999). Analysis of the secondary structure of GehA revealed the presence of 8 β strands and 11 α helices in mature GehA. The 8 β strands found are in agreement with the 8 β strands that form the typical β sheet of lipases (Jaeger *et al.*, 1999), whereas the number of α helices obtained should be considered with care due to the fact that the last four α helices could correspond to just two α helices, since they are short and close, and the model shows a lower confidence in this region. Moreover, an additional α helix and another β strand were present in the signal peptide of GehA (Figure C5.3).

Next page: Figure C5.3 Amino acid sequence and secondary structure prediction of GehA.

AA: amino acid sequence of GehA (signal peptide in green, conserved pentapeptide of lipases in yellow, putative catalytic aminoacids in red). Pred: secondary structure prediction (C: coil – lilac line –; H: α helix – red cylinders –; E: β strand – blue arrows –). Conf: confidence of the secondary structure predicted (from 0 – the lowest confidence – to 9 – the highest confidence –).



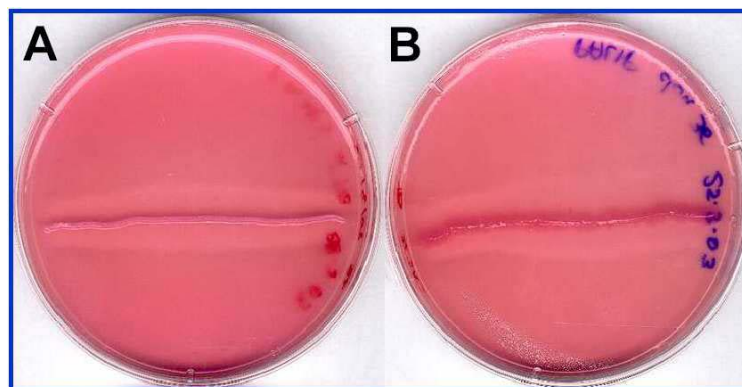
Furthermore, analysis of the secondary structure confirmed that the conserved Gly-His-Ser-Gln-Gly pentapeptide containing the catalytic serine forms a turn between strand $\beta 5$ and the following α helix (Figure C5.3), the so-called “nucleophile elbow”, which is present in all known lipases and constitutes the most conserved structural arrangement of the α/β hydrolase fold (Jaeger *et al.*, 1999; General introduction 2.2.2). Asp²⁶⁷ (located in a turn after strand $\beta 7$) and His²⁹⁷ (located after $\beta 8$) were assigned as the two other members of the catalytic triad of this lipase (Figure C5.3), according to their position with respect to the prototypic α/β hydrolase fold (Jaeger *et al.*, 1999; General introduction 2.2.2).

3.1.2 Characterization of GehA

The lipolytic activity of *E. coli* XL1-Blue-pUC-GehA was detected on lipid-supplemented CeNAN agar plates. Clear hydrolysis zones were observed using tributyrin and triolein as substrates (Figure C5.4), whereas low fluorescence emission was found on plates containing olive oil (not shown).

Figure C5.4 Activity of *E. coli* XL1-Blue-pUC-GehA on lipid substrates.

Degradation haloes of *E. coli* XL1-Blue-pUC-GehA grown on CeNAN agar plates supplemented with tributyrin (A) and triolein (B).



However, zymograms using MUF-derivatives and performed after SDS-PAGE, Native-PAGE and IEF separation of 50-fold concentrated crude cell extracts containing GehA did not show the presence of any activity band, probably due to the low expression and activity of GehA. Moreover, these gels did not show any additional

protein band with respect to those detected in control extracts from *E. coli* XL1-Blue-pUC19. Thus, the MW and pI of GehA could not be experimentally confirmed.

Cell extracts from this clone were also assayed for determine the lipolytic activity of GehA on several *p*-NP- and MUF-derivatives (Table C5.2, Figure C5.4). GehA displayed an intermediate behaviour between “true” lipases and carboxylesterases since it showed preference for acyl groups of medium-chain length, and a similar lower activity on longer and shorter substrates. The highest activity (100%) was found on *p*-NP caprate ($4.7 \cdot 10^{-1} \pm 0.3 \cdot 10^{-2}$ mU mg⁻¹ protein) and on MUF-butyrate ($1.1 \cdot 10^{-2} \pm 0.1 \cdot 10^{-3}$ mU mg⁻¹ protein). Furthermore, GehA efficiently hydrolyzed *p*-NP laurate, whereas it showed a low activity on other *p*-NP derivatives (residual activity 20–40% on the other C_{2–16}-derivatives). *p*-NP stearate and MUF-oleate were the poorer substrates, although their activity with respect to *p*-NP butyrate and MUF-butyrate was about 30–50% (Table C5.2, Figure C5.5).

Table C5.2 Substrate profile of GehA.

Substrate	GehA Activity	
	mU mg ⁻¹ EstV	%
<i>p</i> -NP acetate (C _{2:0})	0.156	32.9
<i>p</i> -NP butyrate (C _{4:0})	0.133	28.1
<i>p</i> -NP valerate (C _{5:0})	0.187	39.5
<i>p</i> -NP caproate (C _{6:0})	0.101	21.4
<i>p</i> -NP caprylate (C _{8:0})	0.169	35.7
<i>p</i> -NP caprate (C _{10:0})	0.473	100.0
<i>p</i> -NP laurate (C _{12:0})	0.292	61.8
<i>p</i> -NP palmitate (C _{16:0})	0.103	21.9
<i>p</i> -NP stearate (C _{18:0})	0.038	8.0
MUF-butyrate (C _{4:0})	0.011	100.0
MUF-oleate (C _{18:1cΔ9})	0.006	51.8

The standard deviations obtained ranged from 2% to 10% of the corresponding mean values. All the substrates were assayed at a concentration of 1 mM, at 37 °C and pH 7.

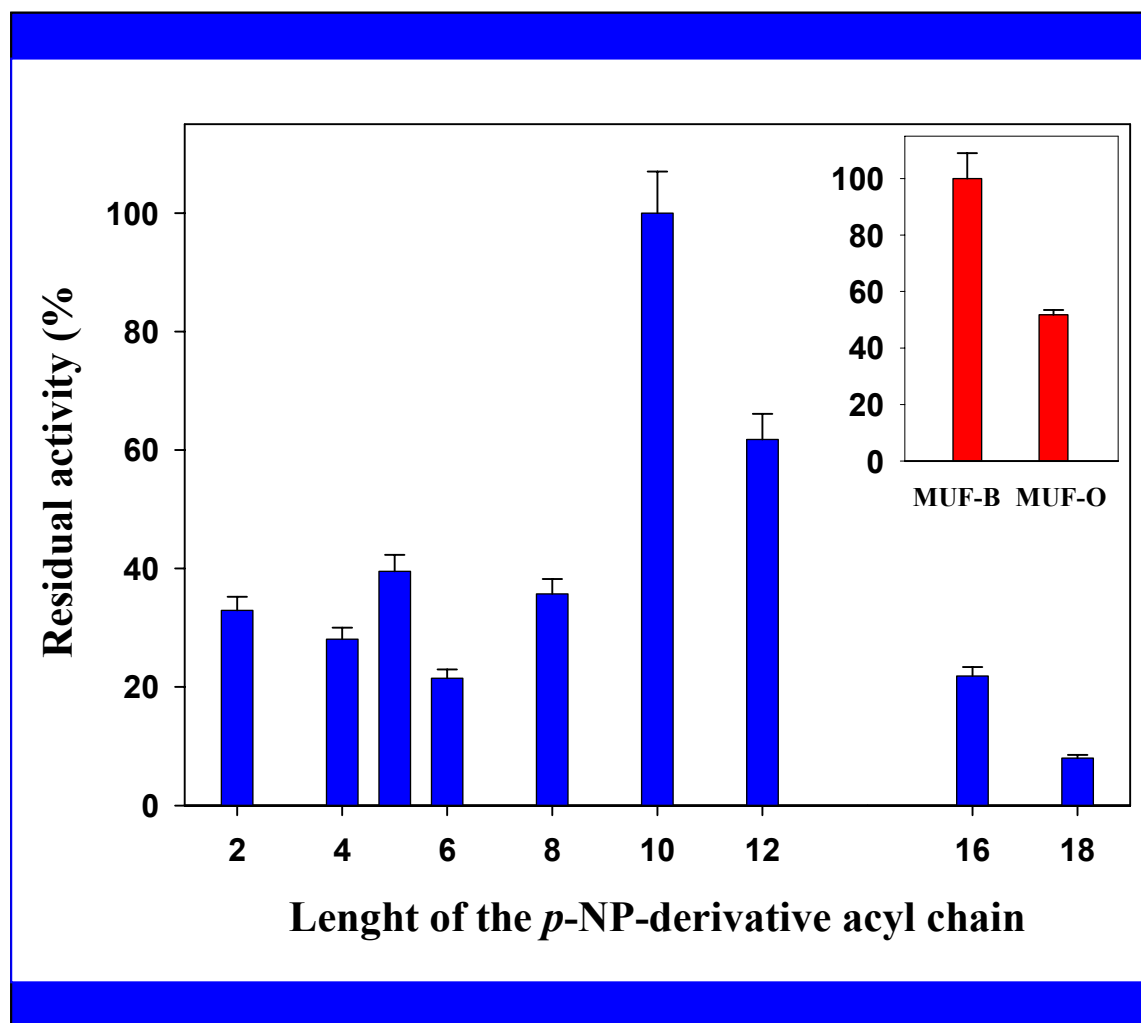


Figure C5.5 Substrate range of GehA.

Relative activity with respect to the maximum activity (activity on *p*-NP caprate) vs. length of the *p*-NP-derivative acyl chain is plotted in blue. Activities on MUF-B (MUF-butyrate – C₄ –; 100%) and MUF-O (MUF-oleate – C₁₈ –) are also compared (in red).

The effect of temperature and pH on the activity of GehA was determined using MUF-butyrate as substrate. The highest activity (100%) on this substrate was found at 37 °C and pH 7. Moreover, GehA activity was higher than 50% from 20 °C to 50 °C, and higher than 50% from pH 5 to pH 7.5 (Figure C5.6). Although a detailed analysis of the stability of GehA was not performed, this enzyme remained active for at least 30 days when it was stored at 4 °C and pH 7.

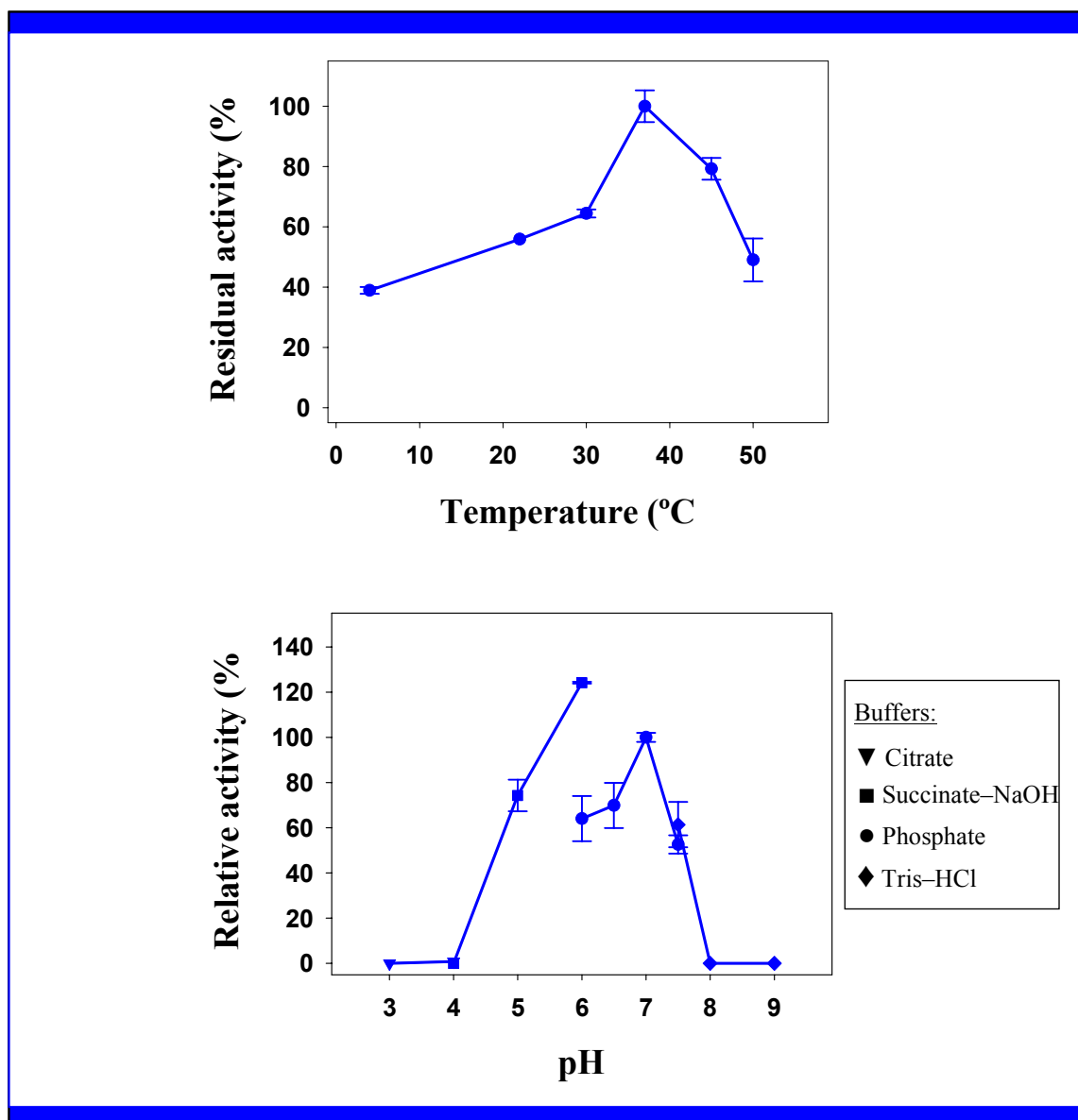


Figure C5.6 Optimum temperature and pH of GehA.

When we analyzed the kinetic behaviour of GehA on *p*-NP butyrate and *p*-NP caprate, the enzyme showed the typical Michaelis-Menten behaviour of carboxylesterases, with no interfacial activation. Moreover, although the V_{\max}^{app} on *p*-NP caprate was nearly 3-fold higher than on *p*-NP butyrate, the K_M^{app} was almost the same, indicating that the affinity of the enzyme for both substrates was similar (Figure C5.7).

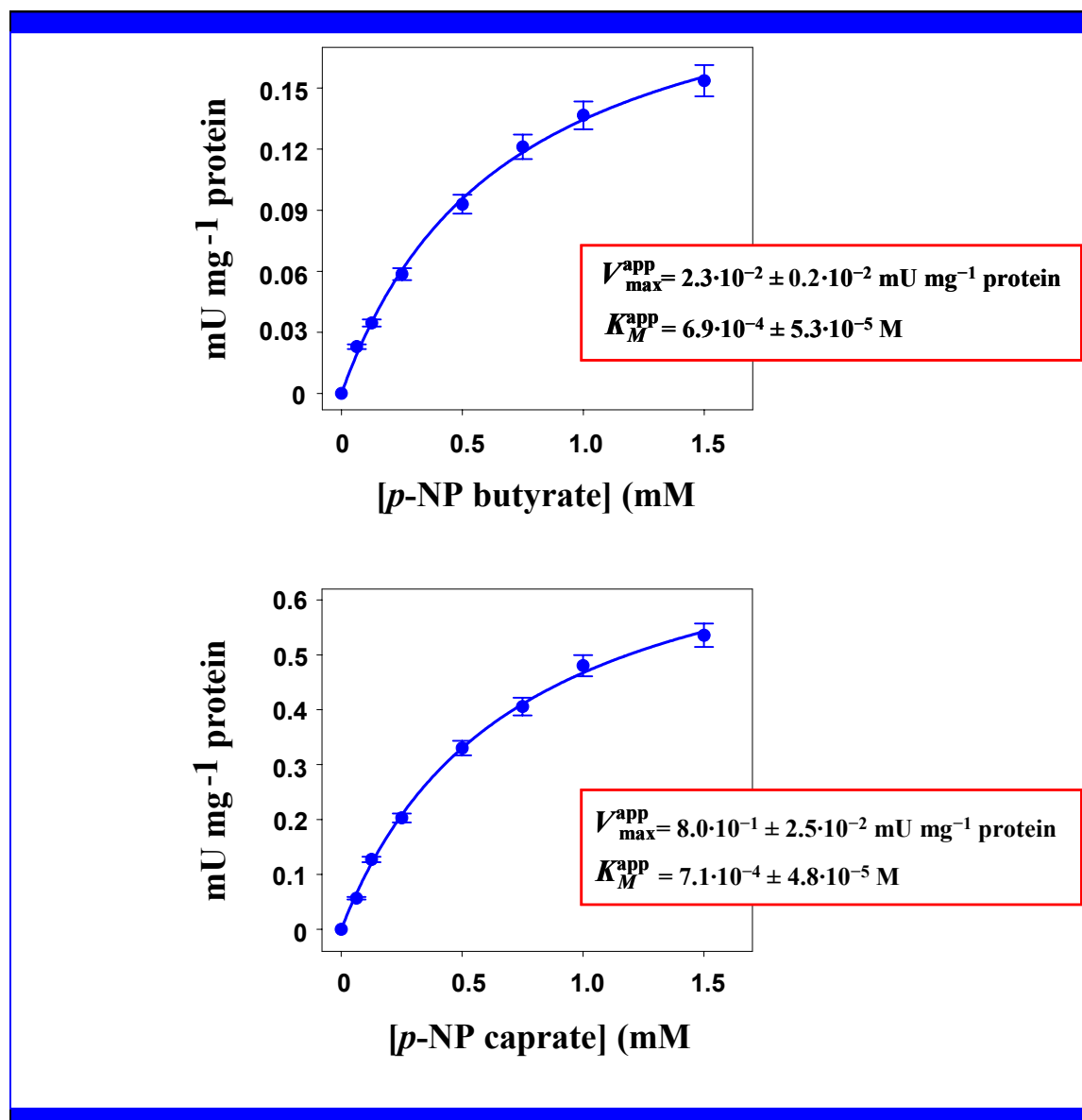


Figure C5.7 Kinetic behaviour of GehA on *p*-NP butyrate and *p*-NP caprate.

The effect of different agents on the activity of GehA was determined using *p*-NP laurate and the results obtained are shown in Table C5.3 and Figure C5.8. Among the cations analyzed, only Ba²⁺ and Co²⁺ caused a significant inhibition of GehA (22.5 and 71.2% residual activity, respectively) at 1 mM, whereas Ag⁺, Ca²⁺, Hg²⁺, Mg²⁺, Ni²⁺ and Pb²⁺ strongly activated GehA (residual activity higher than 125%) at this concentration. When cations were assayed at 10 mM, Ag⁺, Ba²⁺, Co²⁺, Fe²⁺, Ni²⁺ and Zn²⁺ caused a high inhibition (residual activity lower than 10% except for Zn²⁺),

whereas Ca^{2+} , Cu^{2+} , Mg^{2+} and Pb^{2+} strongly activated GehA (residual activity 138–271%) (Table C5.3; Figure C5.8).

The influence of the amino acid-modifying agents NAI (*N*-acetylimidazole; tyrosine), PHMB (*p*-hydroxymercuribenzoic acid; cysteine) and PMSF (phenylmethylsulfonyl fluoride; serine), and the effect of EDTA, urea and SDS were also tested. NAI and PHMB caused a significant reduction of GehA activity at 10 mM, suggesting that cysteine and tyrosine are involved in the functional or structural domains of the cloned enzyme, whereas PMSF was almost inactive. EDTA, urea and SDS were also inactive at 1 mM, although SDS and, mainly, EDTA inhibited GehA at 10 mM (Table C5.3; Figure C5.8).

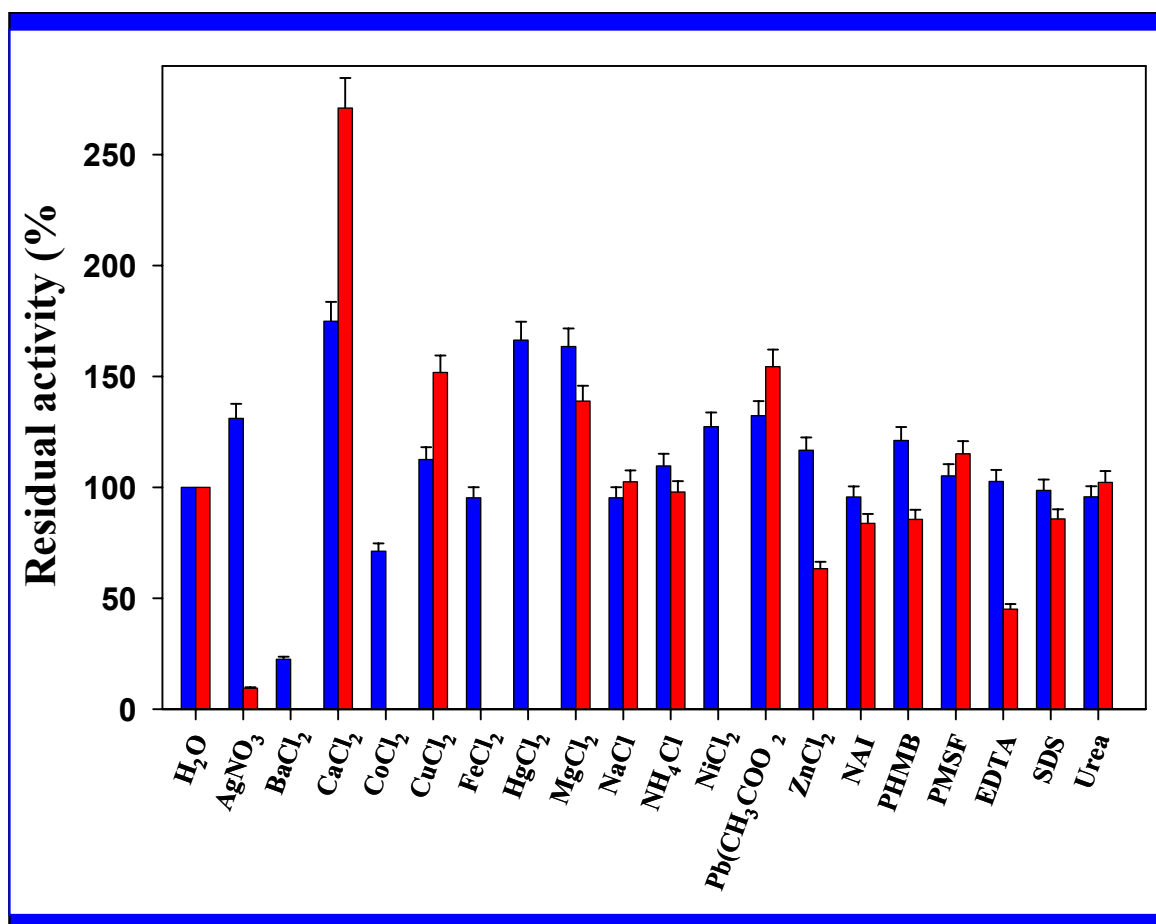


Figure C5.8 Effect on GehA of several agents at a concentration of 1 mM (blue) and 10 mM (red).

Table C5.3 Effect of several agents on GehA.

Agent	Residual activity (% □)	
	1 mM	10 mM
H ₂ O	100.0	100.0
AgNO ₃	131.1	9.4
BaCl ₂	22.5	UD
CaCl ₂	174.9	271.0
CoCl ₂	71.2	UD
CuSO ₄	112.5	151.8
FeCl ₂	95.3	UD
HgCl ₂	166.4	-
MgCl ₂	163.5	138.9
NaCl	95.3	102.5
NH ₄ Cl	109.7	97.9
NiCl ₂	127.4	UD
Pb(CH ₃ COO) ₂	132.3	154.4
ZnCl ₂	116.7	63.3
NAI	95.6	82.8
PHMB	121.1	85.6
PMSF	105.2	115.1
EDTA	102.7	45.1
SDS	98.6	85.8
Urea	95.7	102.2

The standard deviations obtained ranged from 2% to 10% of the corresponding mean values. HgCl₂ could not be assayed at 10 mM by using this method. UD: undetectable activity.

3.2 SELECTION, CLONING AND CHARACTERIZATION OF *H. pylori* 26695 EstV

The selection, cloning and characterization of *H. pylori* 26695 EstV was performed as described in the Materials and Methods and is summarized in figure C5.2.

3.2.1 Selection and analysis of EstV

The genome and proteome of *H. pylori* 26695 were analyzed in order to find out the ORFs from this strain showing similarity to lipases, since the only ORF annotated as a lipase-like protein did not show any similarity to known lipases and did not display the structural features of these enzymes (in fact, it corresponded to a membrane transporter).

For this purpose, the amino acid sequences of the lipases mentioned above were analyzed through BLAST search against the putative proteins of *H. pylori* 26695. From this analysis, HP0289, HP0346, HP0739, HP0906 and Omp26, as well as the previously cloned and characterized PldA phospholipase A1, appeared as the putative proteins with the highest similarity to lipases, or being similar to a major number of known lipases. These putative proteins were re-analyzed through BLAST search against all kind of enzymes, being HP0739 the only one that displayed higher similarity to lipases than to other enzymes. This fact, which was confirmed through ClustalW analysis, and the fact that HP0739 was the only candidate displaying all the typical motifs of lipases, led us to select this putative protein as the best candidate.

Analysis of *H. pylori* 26695 genome revealed that the ORF of *HP0739* gene (AE000586) was 726 bp long (from position 794021 to 794746, both included), with the first nucleotide and the last 15 nucleotides overlapping with the previous and subsequent ORFs. Furthermore, two promoter regions were found in the upstream region of this gene: region 793809–793859 (score 0.99) and region 793909–793958 (score 1 – the maximum –). Moreover, a sequence displaying the typical features of a ribosome binding site (aagaa) located 10 bp upstream of the start codon, as well as

several inverted repeats located 112 bp downstream of the stop codon of *HP0739*, that could act as transcription terminators, were also found.

Protein *HP0739* (AED07785), putatively annotated as a 2-hydroxy-6-oxohepta-2,4-dienoate hydrolase (26.7% BLASTp identity to the epoxide dienoate hydrolase from *Pseudomonas putida* CE2010) by Tomb *et al.* (1997), showed the highest identity (BLASTp) to the hypothetical protein Jhp0676 from *H. pylori* J99 (97% identity) and other putative proteins from related strains such as *Campylobacter jejuni*. *HP0739* showed also a moderate identity (25–40%) to several known and putative lipases from family V of bacterial lipases (Arpigny & Jaeger, 1999) and other lipases and hydrolases, whereas its identity to known dienoate hydrolases was lower than 27%. When ClustalW analyses were performed using non-putative proteins, those showing the highest identity (13–21%) and similarity (35–50%) were the bacterial lipases from family V, and several bacterial lipases from other families such as *Mycoplasma hyopneumoniae* lipase, which is related to lipases from family II (Schmidt *et al.*, 2004), and the carboxylesterase from *Spirulina platensis*, which belongs to family VI (Arpigny & Jaeger, 1999). On the contrary, the dienoate hydrolases from *Pseudomonas putida* CE2010 and other bacterial strains displayed a lower identity to *HP0739*. For this reason, and due to the fact that *HP0739* displayed the typical features of lipases from family V, this protein was preliminarily assigned as a member of family V of bacterial lipases, being named EstV.

Table C5.4 Amino acid composition of EstV.

Ala (A)	15	6.2%	Gly (G)	14	5.8%	Pro (P)	6	2.5%
Arg (R)	6	2.5%	His (H)	10	4.1%	Ser (S)	18	7.5%
Asn (N)	12	5.0%	Ile (I)	12	5.0%	Thr (T)	5	2.1%
Asp (D)	12	5.0%	Leu (L)	31	12.9%	Trp (W)	2	0.8%
Cys (C)	4	1.7%	Lys (K)	26	10.8%	Tyr (Y)	7	2.9%
Gln (Q)	9	3.3%	Met (M)	6	2.5%	Val (V)	14	5.8%
Glu (E)	14	5.8%	Phe (F)	19	7.9%			

- Total number of negatively charged residues (Asp + Glu): **26**
- Total number of positively charged residues (Arg + Lys): **32**
- Short non-polar residues (Ala + Gly + Ileu + Leu + Val) = **86 (35.7%)** □

Analysis of the predicted protein EstV revealed that it corresponded to a protein of 241 amino acids, with a deduced MW of 27527 Da and a theoretical pI of 9.0, and without any sequence displaying the features of a signal peptide. EstV showed also a high content in short non-polar residues (35.7% of the total; Table C5.4), as is described for lipolytic enzymes (Fojan *et al.*, 2000). Furthermore, analysis of the primary structure of this protein revealed that EstV showed the typical Gly-Xaa-Ser-Xaa-Gly pentapeptide of lipases (Gly-His-Ser-Phe-Gly in this case) (Fojan *et al.*, 2000), as well as other conserved motifs of bacterial lipases from family V.

More detailed computational analysis of the amino acid sequence of EstV using 1D, 2D and 3D sequence profiles revealed that it was a globular, compact and single-domain protein, belonging to the group of serine-hydrolases and displaying the typical α/β hydrolase fold of lipases (Jaeger *et al.*, 1999), although a three-dimensional model of this enzyme could not be obtained due to its low similarity to lipases of known structure. The analysis of the secondary structure predicted for EstV (Figure C5.3) revealed the presence in this protein of 8 β strands, in agreement with the 8 β strands that form the typical β sheet of lipases (Jaeger *et al.*, 1999), and 7 α helices (Figure C5.9). Moreover, the Gly-His-Ser-Phe-Gly pentapeptide of EstV containing the catalytic serine (Ser⁹⁹) was found in a turn between strand β 5 and the following α helix (Figure C5.3), forming the typical “nucleophile elbow” present in all known lipases (Jaeger *et al.*, 1999; General introduction 2.2.2). Asp¹⁹² (located in a turn after strand β 7) and His²¹⁹ (located after β 7) were assigned as the two other members of the catalytic triad of this lipase (Figure C5.3), according to their position with respect to the prototypic α/β hydrolase fold (Jaeger *et al.*, 1999; General introduction 2.2.2), and on the basis of sequence alignments with lipases from family V.

In view of the results obtained from sequence alignments and from molecular and structural analyses, the putative lipase EstV was subsequently cloned and characterized in order to confirm its lipolytic activity.

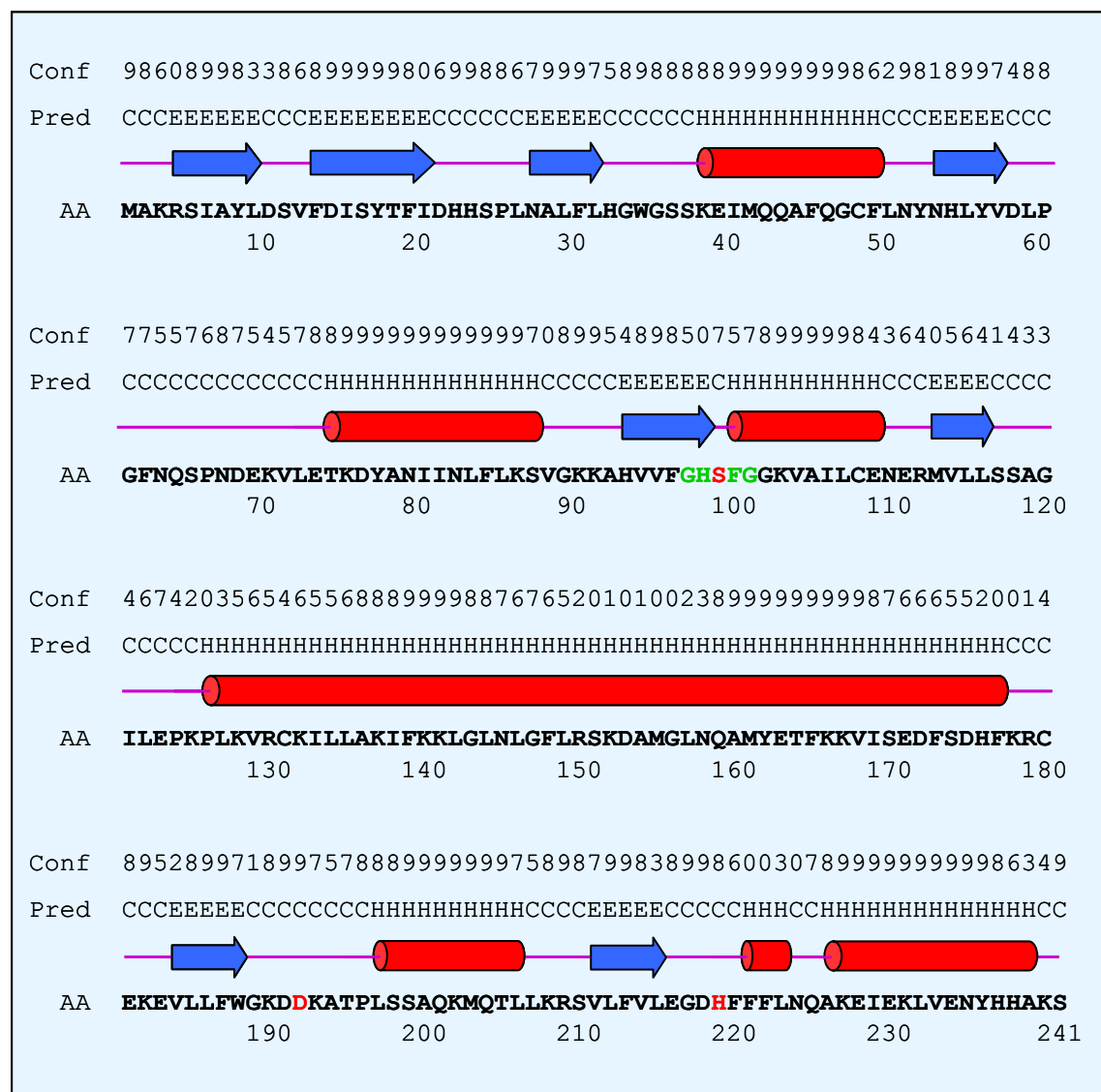


Figure C5.9 Amino acid sequence and secondary structure prediction of EstV.

AA: amino acid sequence of EstV (conserved pentapeptide of lipases containing the catalytic serine in green, putative catalytic amino acids in red). Pred: secondary structure prediction (C: coil –lilac line –; H: α helix – red cylinders –; E: β strand – blue arrows –). Conf: confidence of the secondary structure predicted (from 0 – the lowest confidence – to 9 – the highest confidence –).

3.2.2 Cloning and purification of EstV

As previously stated (Materials and Methods 2.2.2; Figure C5.2), several approaches were used to clone *estV* (HP0739) gene. However, a successful cloning was only achieved by PCR amplification using the primers HPESTFW and HPESTBW,

designed for the specific amplification of *estV* ORF and a few nucleotides of the upstream and downstream regions of this gene, followed by ligation of the resulting 750 bp-amplified DNA fragment (Figure C5.10A) to *Sma*I-digested pUC19 and subsequent transformation into *E. coli* DH5 α . The recombinant clone obtained (*E. coli* DH5 α -pUC-EstV) was analyzed on lipid-supplemented CeNAN agar plates to detect the putative lipolytic activity of EstV. Clear hydrolysis zones were detected using tributyrin as substrate (see Figure C5.2), whereas no activity was found on plates containing olive oil or triolein (not shown). Moreover, crude cell extracts from the recombinant clone displayed activity on MUF-butyrate and MUF-oleate when assayed by the classical fluorimetric liquid assay (1.7 ± 0.1 and $3.2 \cdot 10^{-2} \pm 0.2 \cdot 10^{-2}$ mU mg⁻¹ protein, respectively, after subtraction of the basal activity of the host strain).

Since purification of EstV by the His-tag system was unsuccessful (see Figure C5.2), the clone *E. coli* DH5 α -pUC-EstV was used to perform the purification of EstV protein through FPLC. Maximum lipolytic activity was found in crude cell extracts from cultures induced with 1 mM IPTG at A_{600 nm} of 0.5–0.6, and subsequently incubated overnight. Purification of EstV was achieved after gel filtration (Figure C5.10C), ion exchange and gel filtration chromatography. Purified EstV migrated as a band of ca. 28 kDa on SDS-PAGE gels, and displayed low lipolytic activity on zymograms (Figure C5.10B). However, a low amount of other protein bands appeared in the Coomassie-stained SDS-PAGE gels, indicating that total purification had not been achieved. This fact was confirmed when the N-terminal sequence of the 28 kDa band could not be obtained due to the presence of more than one protein in this band.

Therefore, an additional purification step was performed, consisting in an ion exchange separation followed by a sharp increase in the NaCl concentration of the buffer used (glycine–NaOH, pH 10) to unstick EstV from the column and from a second contaminant protein that could not be removed in the previous steps (Figure C5.10D). This process allowed us to purify EstV almost to homogeneity (215-fold purified with a yield of 19.5% and with a specific activity of 664.1 mU mg⁻¹ protein; Table C5.5). The amount of purified protein obtained was used to perform the biochemical characterization of EstV as well as the inhibition assays by natural substances, but was not enough to confirm the N-terminal sequence of the enzyme.

Table C5.5 Purification of EstV.

Step	Total activity (mU □	Total protein (mg □	Specific activity (mU mg ⁻¹ protein □	Purification fold	Yield (% □
Crude extract	44.0	14.2	3.1	1	100
2 nd ionic exchange + sharp NaCl increase	8.6	1.3·10 ⁻²	667.9	215	19.5

The assays were performed with the new fluorimetric liquid assay, at 50 °C and pH 10, using 1 mM MUF-butyrates as substrate.

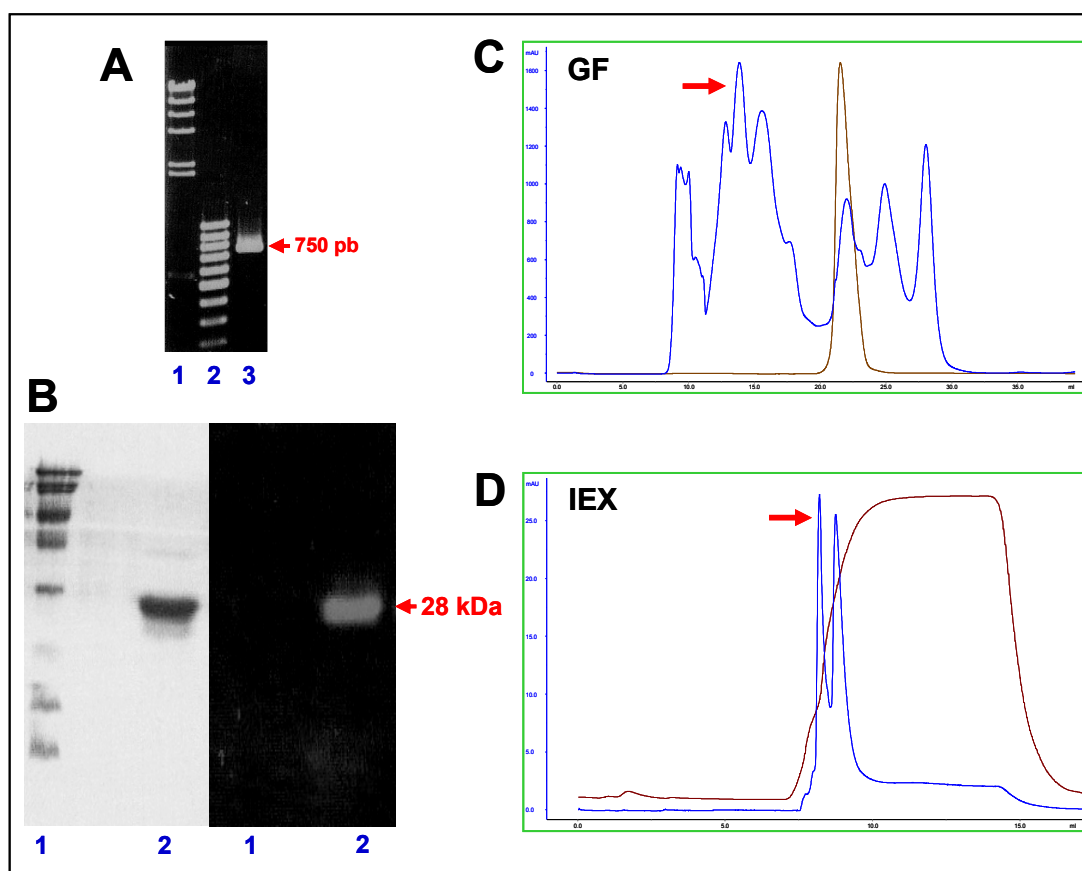


Figure C5.10 Cloning and purification of EstV.

A: amplification using HPESTFW/HPESTBW primers (1: λ DNA/*Hind*III marker; 2: 100 bp Ladder marker, 3: *H. pylori* 26695). B: SDS-PAGE (left) and zymogram using MUF-butyrates as substrate (right) of EstV purified by gel filtration, ion exchange and gel filtration (1: broad-range MW protein marker; 2: EstV purified fraction). C: first purification step of EstV (gel filtration – GF –). D: final purification of EstV by a second ionic exchange (IEX) step followed by a sharp increase in NaCl concentration to unstick EstV from the column and from other undesired proteins. C and D: blue line, protein (the fraction containing EstV is indicated by a red arrow); brown line, salts (C) or NaCl (D) concentration.

3.2.3 Characterization of EstV

With respect to the molecular characterization of EstV, the SDS-PAGE assays followed by zymogram performed to confirm the molecular size (ca. 28 kDa) and activity on MUF-butyrate of EstV after the purification process (see Figure C5.10B), where complemented with zymogram analysis after IEF separation. No additional bands could be observed after Coomassie stain of IEF gels containing purified EstV or 50-fold concentrated cell extracts from *E. coli* DH5 α -pUC-EstV clone. Moreover, any activity bands were obtained after zymogram analysis of these gels using MUF-butyrate, thus, the theoretical pI of EstV could not be experimentally confirmed.

Purified EstV was also tested for determining the lipolytic activity of this enzyme on several *p*-NP- and MUF-derivative substrates (Table C5.6, Figure C5.11).

Table C5.6 Substrate profile of EstV.

Substrate	EstV Activity	
	mU mg ⁻¹ EstV	%
<i>p</i> -NP acetate (C _{2:0})	537.3	100.0
<i>p</i> -NP butyrate (C _{4:0})	478.2	89.0
<i>p</i> -NP valerate (C _{5:0})	396.6	73.8
<i>p</i> -NP caproate (C _{6:0})	242.5	45.1
<i>p</i> -NP caprylate (C _{8:0})	102.5	19.1
<i>p</i> -NP caprate (C _{10:0})	62.9	11.7
<i>p</i> -NP laurate (C _{12:0})	54.3	10.1
<i>p</i> -NP palmitate (C _{16:0})	2.2	0.4
<i>p</i> -NP stearate (C _{18:0})	0.6	0.1
MUF-butyrate (C _{4:0})	667.9	100.0
MUF-oleate (C _{18:1cΔ9})	71.5	10.7

The standard deviations obtained ranged from 2% to 10% of the corresponding mean values. All the substrates were assayed at a concentration of 1 mM. MUF-derivatives were assayed at 50 °C and pH 10, the optima reaction conditions of EstV, whereas *p*-NP-derivatives were assayed at pH 7 and 55 °C (the optimum temperature of EstV at this pH).

EstV displayed the typical behaviour of carboxylesterases since it showed preference for short acyl chains. The highest activity (100%) was found on *p*-NP acetate (537.3 ± 26.9 mU mg⁻¹ EstV at 55 °C and pH 7) and on MUF-butyrate (667.9 ± 15.3 mU mg⁻¹ EstV at 50 °C and pH 10). Furthermore, EstV efficiently hydrolyzed C₄₋₅ *p*-NP-derivatives (residual activity higher than 70%), whereas the activity of this enzyme decreased dramatically (residual activity lower than 20%) on *p*-NP- or MUF-derivatives with acyl chains of 8 or more carbon atoms (Table C5.6, Figure C5.11).

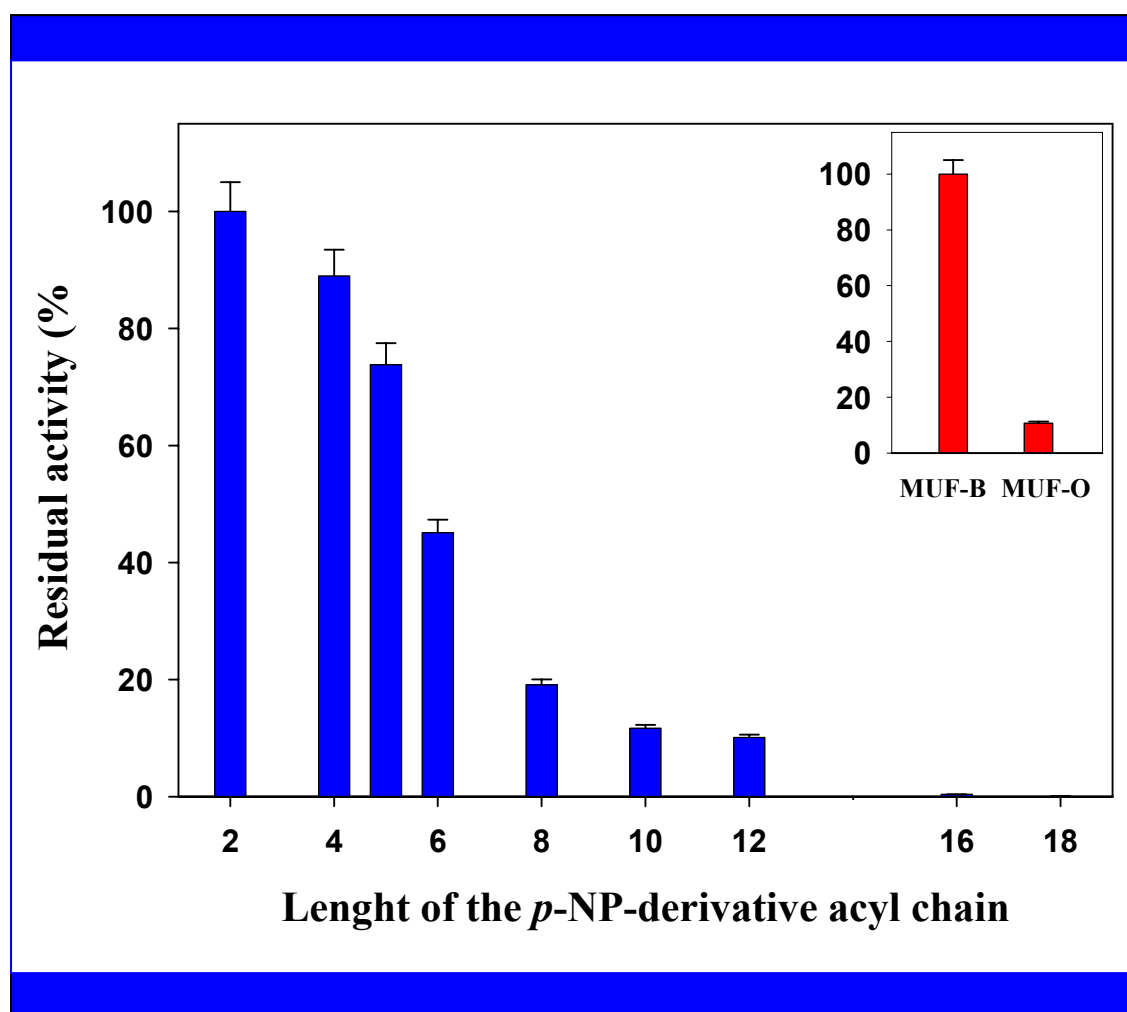


Figure C5.11 Substrate range of EstV.

Relative activity with respect to the maximum activity (activity on *p*-NP acetate) vs. length of the *p*-NP-derivative acyl chain is plotted in blue. Activities on MUF-B (MUF-butyrate – C₄ –; 100%) and MUF-O (MUF-oleate – C₁₈ –) are also compared (in red).

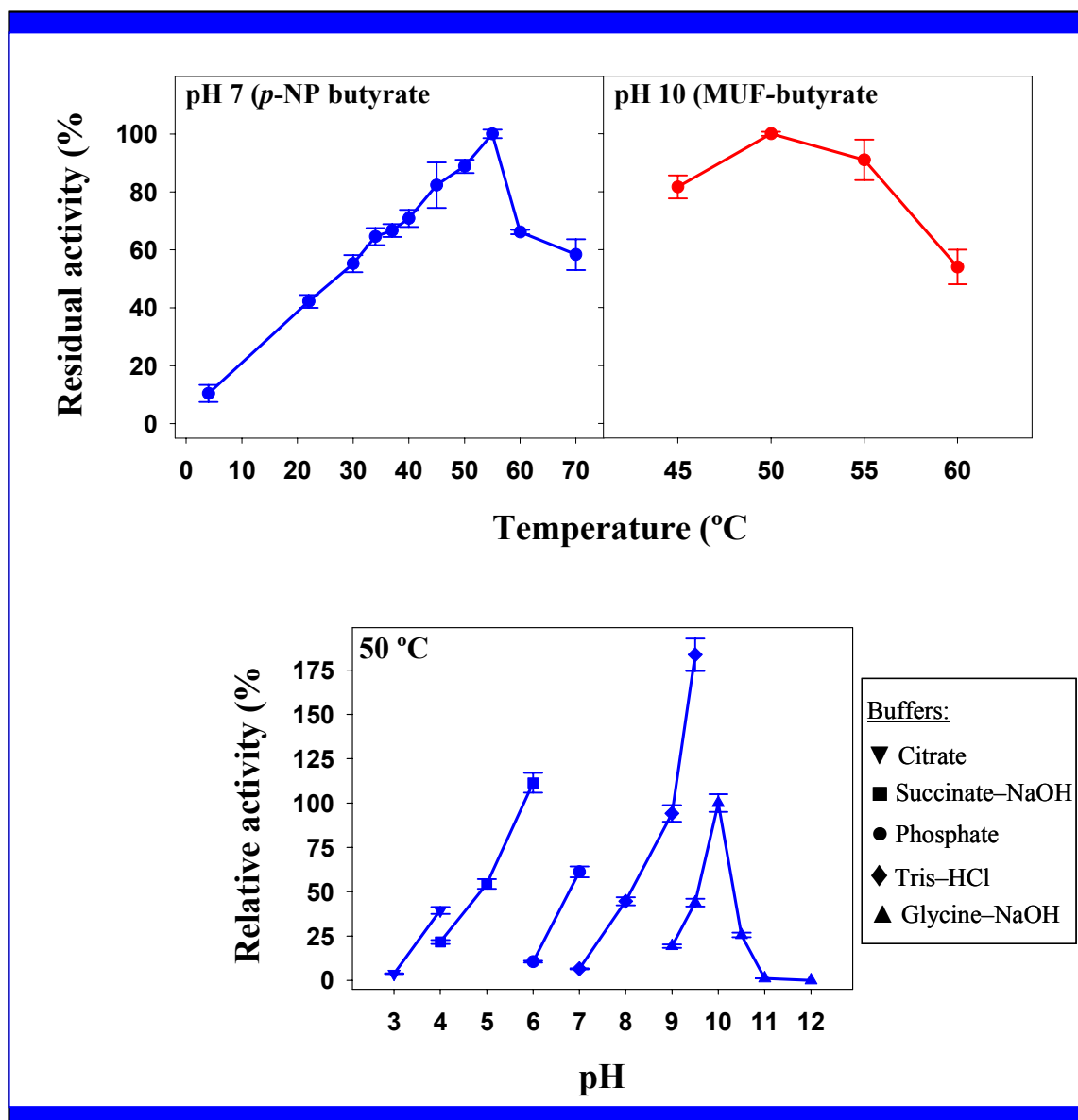


Figure C5.12 Optimum temperature and pH of EstV.

The effect of temperature and pH on the activity of EstV was determined using MUF-butyrate and *p*-NP butyrate as substrates. The highest activity was found at 50 °C and pH 10 using MUF-butyrate as substrate. Moreover, EstV displayed an activity higher than 80% from 45 °C to 55 °C, and over 90% at pH 6 (succinate-NaOH buffer) and at pH 9–9.5 (Tris-HCl), whereas the residual activity was 61.2% at pH 7 (phosphate buffer). When *p*-NP butyrate was used as substrate, the assays were performed at pH 7 to avoid the autohydrolysis of this substrate at pH 10. Interestingly, the optimum temperature was 55 °C under these conditions, whereas the residual

activity was higher than 60% from 34 °C to 60 °C (Figure C5.12). Although a detailed analysis of the stability of EstV was not performed, this enzyme remained active for at least 30 days when it was stored at 4 °C and pH 7 or pH 10.

When we analyzed the kinetics of EstV on MUF-butyrate, the enzyme showed a Michaelis-Menten behaviour with no interfacial activation, as is described for carboxylesterases (Jaeger *et al.*, 1999). A plot with the maximum activity over $1.2 \cdot 10^{-3}$ M, but showing a decreasing activity at higher substrate concentrations was obtained. The plot obtained and the kinetic parameters of EstV calculated from this plot are shown in Figure C5.13.

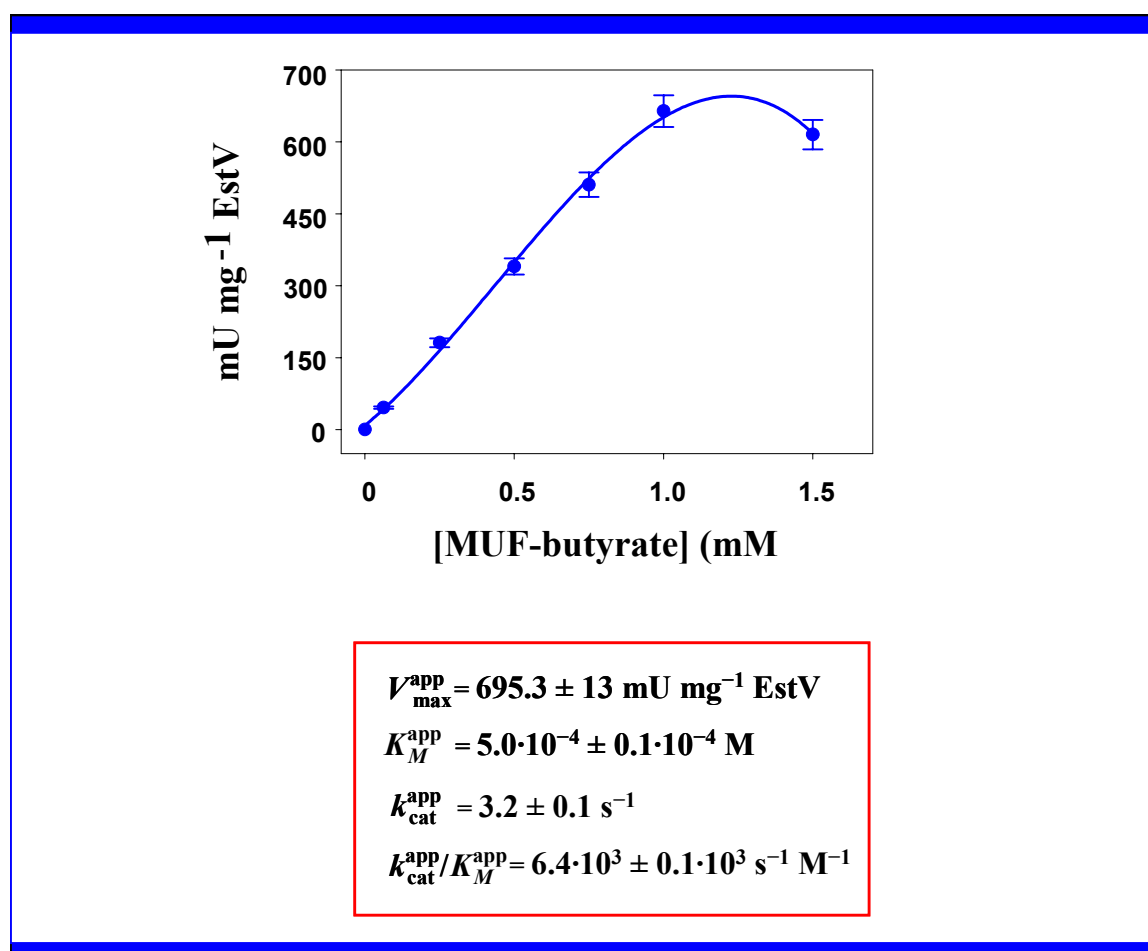


Figure C5.13 Kinetic behaviour of EstV on MUF-butyrate.

The effect of different agents on the activity of EstV was determined (at 55 °C and pH 7) using *p*-NP laurate as substrate, and the results obtained are shown in Table C5.7 and Figure C5.14. Among the cations analyzed, Ag⁺ inhibited almost completely EstV at 1 mM. Hg²⁺ produced also a high inhibition (almost 50%) of this enzyme, whereas Cu²⁺ Pb²⁺ and Zn²⁺ caused a significant inhibition of EstV at this concentration (74–86% residual activity). On the contrary, Ba²⁺, Ca²⁺ and Mg²⁺ activated EstV at 1 mM (residual activity higher than 130%). When cations were assayed at 10 mM, no activity was detected for EstV in the presence of Ag⁺, whereas Cu²⁺ Pb²⁺ and Zn²⁺ caused a high inhibition of this enzyme (residual activity lower than 50%). Co²⁺ and Fe²⁺ produced also a moderate inhibition of EstV at this concentration. On the contrary, Ba²⁺, Ca²⁺ and Mg²⁺ strongly activated EstV at 10 mM (127%, 150% and 135% residual activity, respectively) (Table C5.7; Figure C5.14).

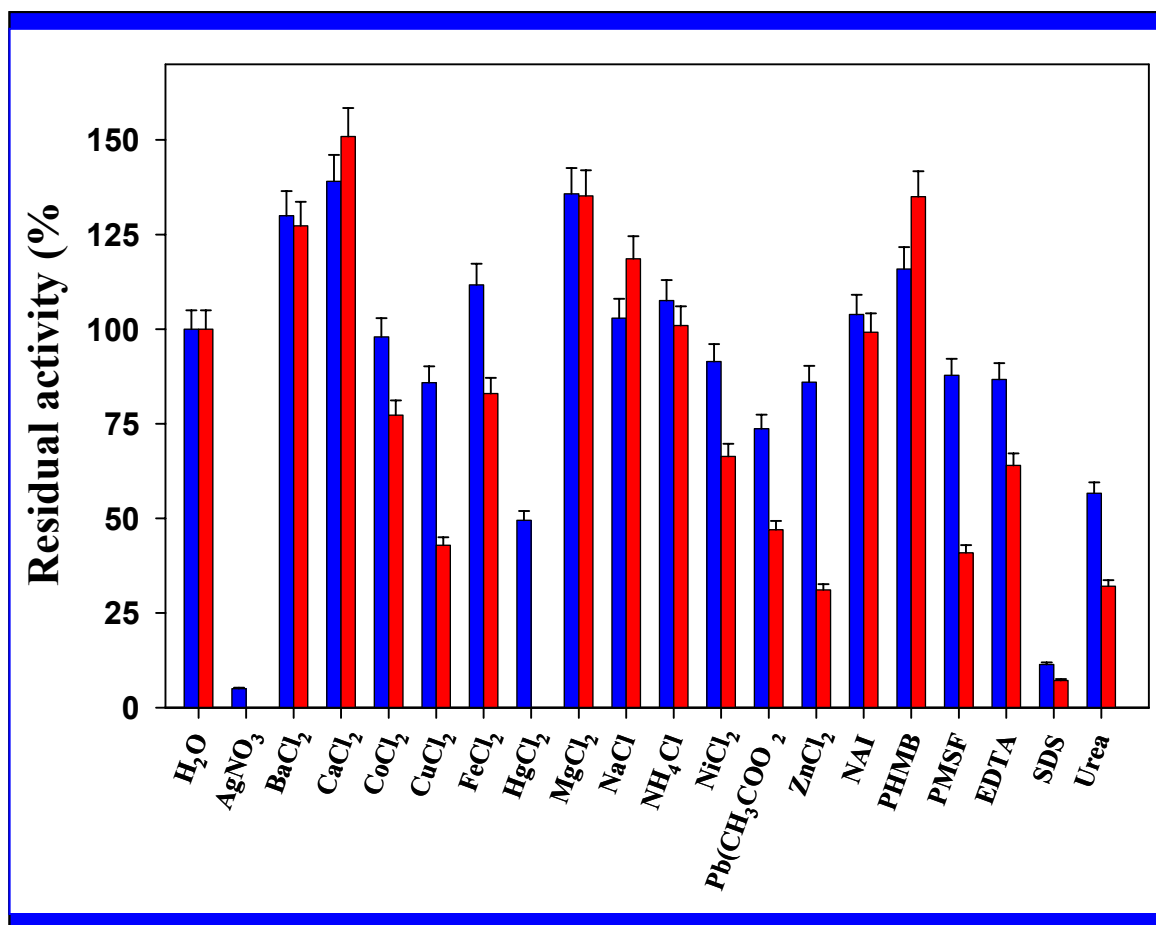


Figure C5.14 Effect on EstV of several agents at a concentration of 1 mM (blue □) and 10 mM (red □)

Table C5.7 Effect of several agents on EstV.

Agent	Residual activity (% □)	
	1 mM	10 mM
H ₂ O	100.0	100.0
AgNO ₃	5.0	UD
BaCl ₂	130.0	127.3
CaCl ₂	139.1	150.9
CoCl ₂	98.0	77.3
CuSO ₄	85.9	42.9
FeCl ₂	111.7	83.0
HgCl ₂	49.5	-
MgCl ₂	135.8	135.2
NaCl	102.9	118.6
NH ₄ Cl	107.6	101.0
NiCl ₂	91.5	66.4
Pb(CH ₃ COO) ₂	73.7	47.0
ZnCl ₂	86.0	31.1
NAI	103.9	99.2
PHMB	115.9	135.0
PMSF	87.8	40.9
EDTA	86.7	64.0
SDS	11.4	7.2
Urea	56.7	32.1

The standard deviations obtained ranged from 2% to 10% of the corresponding mean values. HgCl₂ could not be assayed at 10 mM by using this method. UD: undetectable activity.

The influence of the amino acid-modifying agents NAI (*N*-acetylimidazole; tyrosine), PHMB (*p*-hydroxymercuribenzoic acid; cysteine) and PMSF (phenylmethylsulfonyl fluoride; serine), and the effect of EDTA, urea and SDS were

also tested. PMSF strongly inhibited EstV (41% residual activity at 10 mM), whereas NAI and PHMB caused no significant reduction or even a slight activation of EstV, suggesting that serine, but not cysteine or tyrosine are involved in the functional or structural domains of the cloned enzyme. Among the other agents assayed, SDS produced the strongest inhibition at both 1 mM and 10 mM (11 and 7% residual activity, respectively). Urea caused also a high inhibition of EstV, whereas EDTA produced a lower inhibition of this enzyme (Table C5.7; Figure C5.14).

3.3 INHIBITION OF GehA AND EstV BY NATURAL SUBSTANCES

The results obtained by the colorimetric microassay with respect to the effect on *P. acnes* P-37 GehA and *H. pylori* 26695 EstV of several saponins (β -aescin, digitonin, glycyrrhizic acid – GA – and *Quillaja* saponin – \square S –, flavonoids ((\pm)-catechin and kaempferol) and alkaloids (rescinnamine and reserpine) are shown in Table C5.8 and Figure C5.15.

GehA was strongly inhibited by the flavonoids (\pm)-catechin and kaempferol ($IC_{50} = 2.3\text{--}3.9 \cdot 10^{-4}$ M), whereas GA produced a lower inhibition ($IC_{16} = 4.0 \cdot 10^{-4}$ M) of this enzyme. Digitonin produced a similar inhibition than GA at low concentrations (14.2% inhibition at $4.0 \cdot 10^{-4}$ M and 16% inhibition at $4.1 \cdot 10^{-4}$ M, respectively); however, their inhibition at higher concentrations could not be compared due to the low solubility of digitonin. On the contrary, the other substances analyzed produced almost no effects on this lipase (Table C5.8; Figure C5.15).

EstV was strongly inhibited by reserpine ($IC_{50} = 4.5 \cdot 10^{-5}$ M), whereas β -aescin and GA produced a lower inhibition of this enzyme ($IC_{16} = 2.9\text{--}4.1 \cdot 10^{-4}$ M). Interestingly, (\pm)-catechin and kaempferol produced a moderate (37.2%) and a high (224.3%) activation of EstV, respectively, when assayed at their maximum solubility concentration. On the contrary, digitonin, \square S and rescinnamine caused almost no effect on EstV activity (Table C5.8; Figure C5.15).

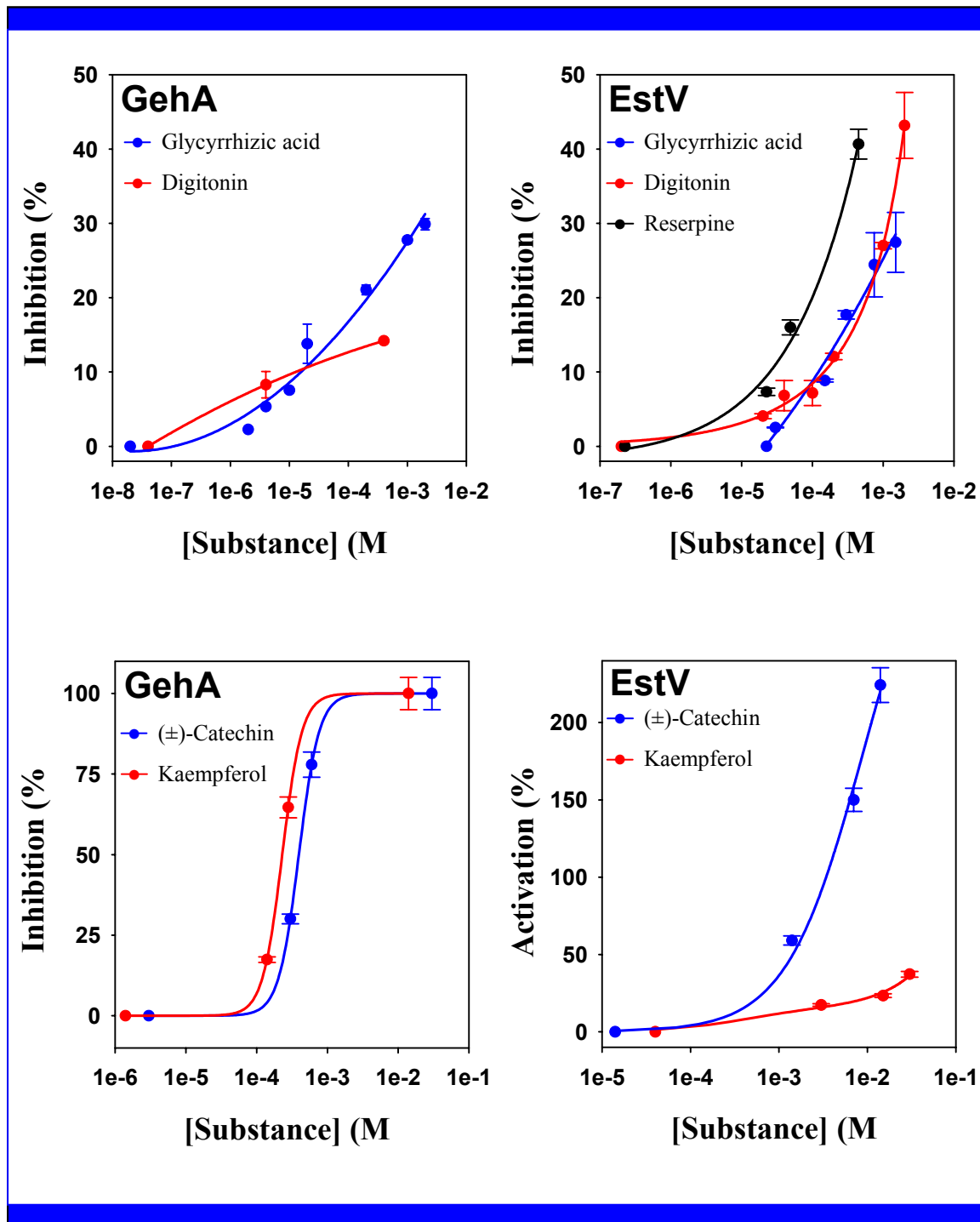


Figure C5.15 Inhibition (and activation) of GehA and EstV by natural substances.

Table C5.8 Effect of natural substances on GehA and EstV.

SUBSTANCE	S_{\max}^* (M□)	<i>P. acnes</i> GehA		<i>H. pylori</i> EstV	
		IC ₁₆ (M□)	IC ₅₀ (M□)	IC ₁₆ (M□)	IC ₅₀ (M□)
I. Saponins					
β-Aescin	$1.5 \cdot 10^{-4}$	> S_{\max}	-	$2.9 \cdot 10^{-4}$	> S_{\max}
Digitonin	$4.0 \cdot 10^{-4}$	~ S_{\max}	-	> S_{\max}	-
Glycyrrhizic acid	$2.0 \cdot 10^{-3}$	$4.0 \cdot 10^{-4}$	> S_{\max}	$4.1 \cdot 10^{-4}$	> S_{\max}
<i>Quillaja</i> saponin	$1.4 \cdot 10^{-3}$	> S_{\max}	-	> S_{\max}	-
II. Flavonoids					
(±)-Catechin	$3.0 \cdot 10^{-2}$	$2.3 \cdot 10^{-4}$	$3.9 \cdot 10^{-4}$	> S_{\max}	-
Kaempferol	$1.4 \cdot 10^{-2}$	$1.4 \cdot 10^{-4}$	$2.3 \cdot 10^{-4}$	> S_{\max}	-
III. Alkaloids					
Rescinnamine	$8.0 \cdot 10^{-4}$	> S_{\max}	-	> S_{\max}	-
Reserpine	$4.5 \cdot 10^{-4}$	> S_{\max}	-	$4.9 \cdot 10^{-5}$	> S_{\max}

*Highest concentration at which each substance was tested.

The assays were performed by colorimetric microassay (37 °C and pH 7), using 1mM *p*-NPL as substrate.

The inhibition produced by natural substances on GehA and EstV was also compared to that produced by these compounds on *C. rugosa* lipase (CRL) (Figure C5.16). Only half of the compounds active on CRL were also active on GehA and EstV. In general, the compounds analyzed produced a very different inhibition on the three lipases, with the exception of GA. On the contrary, β-aescin was only active on CRL and EstV (EstV-IC₁₆ 5-fold higher than CRL-IC₁₆; IC₅₀ only reached on CRL), whereas digitonin was only active on CRL and GehA (GehA-IC₁₆ 5-fold higher than CRL-IC₁₆, IC₅₀ only reached on CRL) and □S was only active on CRL. The highest differences were found for flavonoids. Both (±)-catechin and kaempferol produced a moderate inhibition on CRL, whereas they produced a moderate inhibition of GehA at low concentrations, but a very strong inhibition at higher concentrations (GehA-IC₁₆ 2–4-fold lower than CRL-IC₁₆, but GehA-IC₅₀ 30–45-fold lower than CRL-IC₅₀). However, these flavonoids produced a moderate activation (37%, (±)-catechin) and a very strong activation (220%, kaempferol) on EstV at their maximum solubility concentration.

Significant differences were also found for alkaloids, since rescinnamine (one of the inhibitors most active on CRL) was inactive on both GehA and EstV. Reserpine produced an IC_{16} twice lower on CRL than on EstV, although it produced a higher inhibition of CRL at higher concentrations (IC_{50} only reached on CRL). However, this compound was almost inactive on GehA.

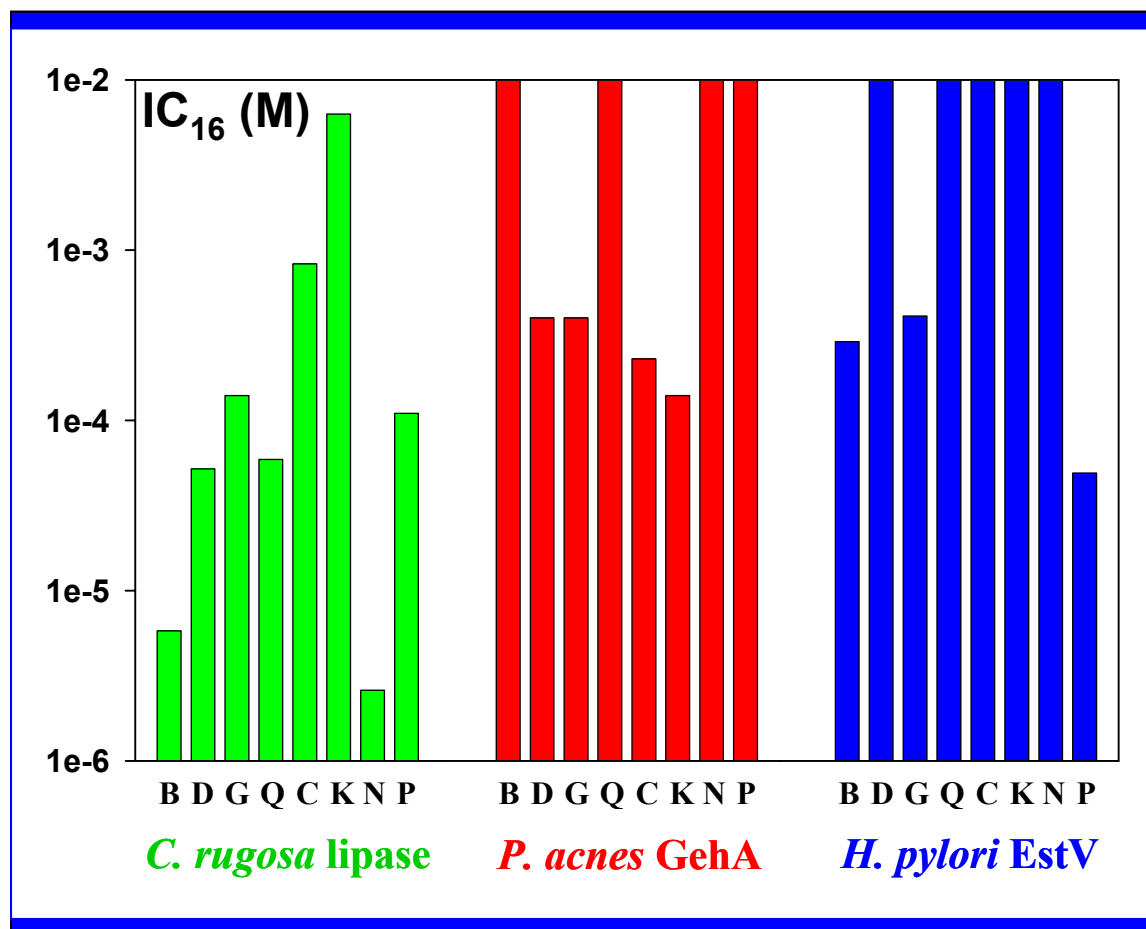


Figure C5.16 Comparison of inhibition by natural substances on CRL, GehA and EstV.

The concentrations producing a 16% inhibition (IC_{16}) on CRL activity (green), *P. acnes* GehA activity (red) and *H. pylori* EstV activity (blue) are compared for several saponins, flavonoids and alkaloids, since the IC_{50} was not reached in most of them. The values given for CRL were obtained by colorimetric microassay (saponins) and by HPLC (flavonoids and alkaloids), whereas values for GehA and EstV were obtained by colorimetric microassay. The substances are plotted in the following order (from left to right): β -aescin (B), digitonin (D), glycyrrhizic acid (G), *Quillaja* saponin (□), (\pm)-catechin (C), kaempferol (K); rescinnamine (N), reserpine (P). The compounds being inactive are plotted as bars reaching the top of the graph.

4 DISCUSSION

4.1 CLONING AND CHARACTERIZATION OF *P. acnes* P-37 GehA

Propionibacterium acnes lipase is considered a major etiological agent in the pathogenesis of acne (Higaki, 2003; General Introduction 3.4.1). For this reason, *P. acnes* P-37 GehA lipase, an enzyme previously cloned and overexpressed (Miskin *et al.*, 1997), and belonging to subfamily I.7 of bacterial lipases (Jaeger & Eggert, 2002), has been cloned and characterized in more detail in this work.

Analysis of the predicted protein GehA confirmed that it was a protein of 339 amino acids and 36 kDa, possessing an N-terminal signal peptide of 26 residues whose cleavage yielded a mature protein of 33 kDa, as previously described (Miskin *et al.*, 1997), and revealed an acid pI (6.59) for this enzyme.

Computational analysis of GehA amino acid sequence revealed that this enzyme is a globular, compact and single-domain protein of the group of serine-hydrolases displaying the typical features of lipases: (1) high content in short non-polar residues, (2) an α/β hydrolase fold with 9–11 α helices and a β sheet constituted of 8 β strands, (3) a catalytic triad constituted by the amino acids Ser¹⁶⁹, Asp²⁶⁷ and His²⁹⁹, each one located at its corresponding position of the prototypic α/β hydrolase fold, and (4) a GHS□G pentapeptide containing the catalytic serine and forming the “nucleophile elbow”, the responsible for the optimal orientation and stabilization of the catalytic serine of all known lipases, and being the most conserved structural arrangement of the α/β hydrolase fold (Jaeger *et al.*, 1999; Fojan *et al.*, 2000; General introduction 2.2.2).

Production of active GehA was achieved by cloning of *gehA* in *E. coli* followed by overexpression of GehA at low temperature and using saccharose-supplemented culture media to avoid the formation of insoluble aggregates. The expression of GehA obtained allowed us to perform the biochemical characterization and inhibition assays of this enzyme. However, it was not enough to perform the molecular characterization of GehA, since no additional protein or activity bands could be detected after cell

extracts separation on SDS-PAGE, Native-PAGE or IEF gels, or in their corresponding zymograms.

The biochemical characterization of GehA revealed that this enzyme displayed an intermediate behaviour between “true” lipases and carboxylesterases. When natural substrates were analyzed, GehA was active on tributyrin, triolein and olive oil, in agreement with results previously reported (Hassing, 1971; Fulton *et al.*, 1974; Pablo *et al.*, 1974; Ingham *et al.*, 1981). Using *p*-NP- and MUF-derivatives, GehA showed preference for medium-chain acyl groups, and a similar lower activity on longer and shorter substrates, being the highest activity achieved on *p*-NP caprate and MUF-butyrate, respectively. Analysis of the kinetic behaviour of this enzyme on *p*-NP butyrate and *p*-NP caprate revealed that the enzyme showed a typical Michaelis-Menten behaviour with no interfacial activation, as is described for carboxylesterases and a few “true” lipases (Verger, 1997; Jaeger *et al.*, 1999). Interestingly, the enzyme showed a similar affinity for both substrates despite of displaying an activity much higher on *p*-NP caprate than on *p*-NP butyrate. All these data can not be directly compared to previous results, since GehA activity on these derivatives is described here for the first time, with the exception of activity on *p*-NP acetate (Fulton *et al.*, 1974). Nevertheless, these results are in agreement with the activity of GehA in a wide range of triacylglycerols (tributyrin, trilaurin, tricaprylin, trimyristin, tripalmitin, tristearin and triolein) previously reported (Hassing, 1971; Fulton *et al.*, 1974; Pablo *et al.*, 1974; Ingham *et al.*, 1981). Moreover, the considerable activity of GehA on C₂₋₁₈ substrates is also in agreement with the wide range of lipids found in human skin (Downie *et al.*, 2004).

When the effect of temperature and pH was analyzed, GehA showed the highest activity at 37 °C and pH 7, displaying also a high activity (more than 50%) from 20 °C to 50 °C, and from pH 5 to pH 7.5. These results are in agreement with those previously reported (Fulton *et al.*, 1974; Ingham *et al.*, 1981), and with the fact that GehA is a secreted enzyme acting on lipids of sebaceous glands under acid-neutral pH conditions and at 37 °C.

The effect of different agents on the activity of GehA was also determined. Among the cations analyzed, Ag⁺, Ba²⁺, Co²⁺, Fe²⁺, Ni²⁺ (at 10 mM) and Zn²⁺ caused a

significant inhibition of GehA. Ag^+ (at 10 mM), Ca^{2+} , Hg^{2+} , Mg^{2+} , Ni^{2+} (at 1 mM) and Pb^{2+} activated GehA, and the other cations analyzed had no effect. Activation by Ca^{2+} (very strong) as well as low inhibition by Zn^{2+} are in agreement with previous results (Weaber *et al.*, 1971; Rebello *et al.*, 1986), whereas the effect of the other cations analyzed has not been described before, to our knowledge, but is in agreement with the general effects of these compounds on other lipases (Gupta *et al.*, 2004; General Introduction 3.4.1).

Among the other agents analyzed, the amino acid-modifying agents NAI and PHMB inhibited GehA activity at 10 mM, suggesting that cysteine and tyrosine are involved in the functional or structural domains of the cloned enzyme. On the contrary, the serine-inhibitor PMSF was inactive, as previously described (Fulton *et al.*, 1974). The lack of GehA inhibition by PMSF could seem surprising since serine is one of the catalytic amino acids of this enzyme, and could be related to a lack of ability of PMSF to fit into the active site of this enzyme. In fact, not all lipases are inhibited by this compound (Gupta *et al.*, 2004). GehA activity was also inhibited by EDTA, as previously described (Weaber *et al.*, 1971), and by SDS (slightly). On the contrary, this lipase was resistant to denaturation by urea, a component of skin and sweat, confirming the adaptation of GehA to the conditions found in the sebaceous glands and the skin.

4.2 SELECTION, CLONING AND CHARACTERIZATION OF *H. pylori* 26695 EstV

H. pylori lipase activity has been related to peptic ulcer since it could hydrolyze the endogenous lipids of the stomach and duodenum lining weakening the barrier properties of mucus, disrupting epithelial cells and generating cytotoxic and pro-inflammatory lipids (Tsang & Lam, 1999; General Introduction 3.4.2). For this reason, we have cloned and characterized a lipolytic enzyme from *H. pylori* 26695.

Since no lipases from this bacterium had been isolated, cloned or characterized in detail before, we analyzed the genome and deduced proteome of *H. pylori* 26695 in

order to select those putative ORFs which could be responsible for the lipolytic activity of this microorganism. After search of *H. pylori* ORFs similar to the lipases mentioned in the Materials and Methods, confirmation of their higher similarity to lipases than to other enzymes, and subsequent search in these ORFs of typical lipase motifs, the ORF HP0739 was selected as the best lipase candidate of *H. pylori* 26695.

HP0739, putatively annotated as a 2-hydroxy-6-oxohepta-2,4-dienoate hydrolase by Tomb *et al.* (1997), showed the highest identity to putative proteins with no assigned function from related strains such as Jhp0676 from *H. pylori* J99. Among the non-putative proteins, those showing the highest identity to HP0739 were the bacterial lipases from family V (Arpigny & Jaeger, 1999) and the lipases from *Mycoplasma hyopneumoniae* (related to family II; Schmidt *et al.*, 2004) and *Spirulina platensis* (family VI; Arpigny & Jaeger, 1999), whereas its similarity to *Ps. putida* dienoate hydrolase (an enzyme involved in the degradation pathway of aromatic compounds such as toluene; Ohta *et al.*, 2001) and similar enzymes was lower. In fact, it is known that lipases from this family share significant amino acid sequence similarity to various bacterial non-lipolytic enzymes such as epoxide hydrolases, dehalogenases and haloperoxidases, which also possess the typical α/β hydrolase fold and catalytic triad (Arpigny & Jaeger, 1999). Therefore, HP0739 was preliminarily assigned as a member of family V of bacterial lipases, being named EstV.

Analysis of the amino acid sequence of EstV showed that it corresponded to a protein of 241 amino acids, with a deduced MW and pI of 27.5 kDa and 9.0, respectively, and without signal peptide. In addition, computational analysis revealed that the predicted protein EstV is a globular, compact and single-domain protein of the group of serine-hydrolases which displays the most common features of lipases: (1) elevated content in short non-polar residues, (2) a typical α/β hydrolase fold constituted by 7 α helices and a β sheet made up of 8 β strands, (3) a catalytic triad that involves the residues Ser⁹⁹, Asp¹⁹² and His²¹⁹, which are located at their prototypic positions of the α/β hydrolase fold, and (4) a typical “nucleophile elbow” constituted by the GHSPG pentapeptide, that contains the catalytic serine, arranged in a turn between strand β 5 and the following α helix (Jaeger *et al.*, 1999; Fojan *et al.*, 2000; General introduction 2.2.2).

In view of the results obtained, EstV was subsequently cloned and purified almost to homogeneity in order to confirm its lipolytic activity, and to perform the characterization and inhibition assays of the enzyme. With respect to the molecular characterization of EstV, the MW but not the pI of the enzyme could be confirmed by SDS-PAGE and IEF followed by zymogram analysis.

The biochemical characterization of EstV revealed that this enzyme was active on tributyrin but not on triolein or olive oil. Moreover, it showed a marked preference for short-chain *p*-NP- and MUF-derivatives (the highest activity was found on *p*-NP acetate), whereas it was poorly active on medium- or long-chain derivatives. In addition, analysis using MUF-butyrate as substrate revealed that EstV displayed a Michaelis-Menten behaviour with absence of interfacial activation. Therefore, EstV was assigned as carboxylesterase, since it displayed the typical substrate preference and kinetic behaviour of these enzymes (Jaeger *et al.*, 1999). This assignation is in agreement with the fact that most lipases of family V are also considered as carboxylesterases (Arpigny & Jaeger, 1999).

When the effect of temperature and pH was analyzed, EstV showed the highest activity at 50 °C and pH 10, displaying also a high activity from 45 °C to 60 °C, and at pH 6 and 9–9.5. Moreover, EstV displayed moderate activity at 37 °C and pH 7. Such optima conditions could seem surprising for an enzyme from an acid-tolerant neutralophile bacterium adapted to a host whose temperature is 37 °C. Nevertheless, these results are similar to those obtained by Weitkamp *et al.* (1993) for the phospholipase C activity of *H. pylori* (maximum activity at 56 °C and pH 8). Furthermore, we should consider that the intracellular pH of *H. pylori* displays a high variability in response to pH changes of its environment (e.g. at pH 7.4 the intrabacterial pH is 8.1, although it can rise in the presence of urea; Wen *et al.*, 2003).

From the results obtained in the biochemical characterization of EstV, it seems that this enzyme would not be the main responsible for the lipolytic activity of *H. pylori* detected by Slomiany *et al.* (1989a). However, both results are difficult to compare since the assays were performed under very different conditions and using different strains. On the one hand, lipase activity reported by these authors was attributed to an extracellular lipase, whereas EstV did not show the presence of a signal peptide.

However, it should be considered that Slomiany *et al.* (1989a), used as enzyme source the filtrate of a saline solution used to wash plates containing *H. pylori* colonies grown from different clinical isolates, a method that can break the cells and release intracellular proteins. Moreover, it should be also considered that EstV could bear a signal peptide not detected by the software we used, which could explain the unsuccessful purification of this protein by the His-tag system, or could be secreted by a mechanism independent from the presence of a signal peptide, as some Gram-negative lipases lacking a typical N-terminal signal sequence but being secreted by the ABC system (Eggert & Jaeger, 2002). On the other hand, these authors report an optimum temperature and pH of 37 °C and 7.2, respectively, results significantly different from those obtained for the cloned enzyme, although EstV displayed also high activity under these conditions. However, it should be taken into account that the assays performed by these authors were carried out using thin layer-chromatography method and ³H-labeled triolein as substrate, and were performed in a temperature range of 20–45 °C and in a pH range of 6–8. Moreover, these authors did not report any data about the substrate preference and enzyme kinetics of the lipase activity of their filtrates, which did not allow a complete comparison with our characterization results. Therefore, it seems that the lipase activity found by these authors could mainly correspond to another of the lipase candidates found in the screening of *H. pylori* proteome, or to another protein not selected during our analysis. On the contrary, EstV could be responsible for the *H. pylori* carboxylesterase activity detected by Mendz *et al.* (1993) using ¹⁹F NMR spectroscopy to analyze the hydrolysis of ethyl fluoroacetate and dimethyl fluoromalonate produced by *H. pylori* cell suspensions. In fact, these authors obtained the maximum activity on ethyl fluoroacetate, which would be in agreement with the maximum activity on *p*-NP acetate obtained for EstV in this work.

The biochemical characterization of EstV was completed by measuring the effect of different agents on the activity this enzyme. Among the cations analyzed, Ag⁺, Co²⁺, Cu²⁺, Fe²⁺, Hg²⁺, Pb²⁺ and Zn²⁺ caused a significant inhibition of EstV, and Ba²⁺, Ca²⁺ and Mg²⁺ activated EstV, which is in agreement with the general effects of these compounds on other lipases (Gupta *et al.*, 2004; General Introduction 3.4.1). PMSF strongly inhibited EstV, whereas NAI and PHMB caused no significant reduction or even activation of EstV, suggesting that serine, but not cysteine nor tyrosine are

involved in the activity of this enzyme. Among the other agents assayed, EDTA produced a low inhibition of this enzyme, whereas SDS and urea produced a very strong inhibition of EstV, which could explain the low activity of EstV on zymograms performed after SDS-PAGE or IEF separation.

4.3 INHIBITION OF GehA AND EstV BY NATURAL SUBSTANCES

The importance of GehA in acne development and the potential role of EstV in *H. pylori*-related ulcers and other diseases led us to analyze the effect on these enzymes of the natural substances producing the highest inhibition on *C. rugosa* lipase (CRL) (Table C5.8; Figure C5.15).

Comparing the results obtained for these lipases to those obtained for CRL, we can see that, in general, the compounds analyzed produced a very different inhibition on the three lipases, mainly between GehA and EstV. GA was the only substance that caused a similar inhibition among all three enzymes, whereas β -aescin was active on CRL and EstV, digitonin was active on CRL and GehA, and \square S was only active on CRL. (\pm)-Catechin and kaempferol displayed the highest differences since they inhibited CRL and GehA and activated EstV. Among the alkaloids analyzed, rescinnamine caused a strong inhibition on CRL, but was inactive on both GehA and EstV, whereas reserpine was active on CRL and EstV, but was almost inactive on GehA. These differences are probably related to the biochemical and structural differences existing among the enzymes analyzed (see General Discussion for a more detailed explanation).

Considering each lipase separately, interesting results were found. *P. acnes* GehA was strongly inhibited by the flavonoids (\pm)-catechin and kaempferol and was moderately inhibited by glycyrrhizic acid (GA) and digitonin, whereas the other substances analyzed produced almost no effects on this lipase. The inhibition produced by these compounds would explain the high anti-GehA and antiacne properties of kampo compositions containing *Glycyrrhizae radix*, a plant rich in GA and flavonoids

(Higaki, 2003). Up to present, it was thought that the beneficial effects of GA and flavonoids was produced by their anti-inflammatory properties, and due to their inhibition of *P. acnes* growth, which in turn would lead to a reduction in lipase activity (Higaki, 2003). However, the results obtained in this work seem to indicate that their therapeutic effect is also tightly connected to their inhibitory activity on *P. acnes* lipase, mainly for the strong GehA inhibitors (\pm)-catechin and kaempferol. Therefore, the wide antiacne effects of these substances, combined with their low toxicity (see General Introduction 4.2.1 and 4.2.2), make them very suitable candidates for the treatment of acne and other *P. acnes*-related diseases. Moreover, these compounds are poorly absorbed (Milgate & Roberts, 1995; Di Carlo *et al.*, 1999), which would reduce their side effects when administrated as topical agents, although it would be a problem for oral treatments. Anyhow, further *in vivo* experiments are necessary to confirm the pharmacological potential of the mentioned substances.

H. pylori EstV was strongly inhibited by reserpine, was moderately inhibited by β -aescin and GA and was activated by (\pm)-catechin and kaempferol, whereas the other substances analyzed had no effect on EstV activity. Reserpine has no potential use in the treatment of ulcer since it is ulcerogenic (La Barre, 1960). With respect to flavonoids, the activation of EstV produced by (\pm)-catechin and kaempferol indicate that their antiulcerogenic activity, previously attributed to gastroprotective and anti-inflammatory effects, to inhibition of *H. pylori* growth, etc (Beil *et al.*, 1995; General Introduction 4.2.2), is not related to EstV activity. However, it could be also possible that an increased activity of EstV was detrimental for *H. pylori*.

On the contrary, β -aescin and GA are very interesting candidates for the therapy of *H. pylori* related-ulcers because they inhibit *H. pylori* EstV and display several antiulcer effects. For example, β -aescin produces inhibition of gastric acid and pepsinogen secretion (Marhuenda *et al.*, 1993), as well as an improvement of blood flow (Marhuenda *et al.*, 1994), whereas GA, or its corresponding sodium and potassium salts produced by the intestinal microflora, have gastro-protective effects, inhibit *H. pylori* growth (Kim *et al.*, 2000) and inhibit *H. pylori* N-acetyl transferase activity (Chung, 1998). Moreover, carbenoxolone, a derivative from GA, accelerates peptic ulcer healing probably by enhancing the rate of incorporation of various sugars into gastric mucosal glycoproteins, stimulating thus gastric mucus production. This

compound seems also to promote mucosal cell proliferation, inhibit mucosal cell exfoliation, inhibit prostaglandin degradation, increase the release of PGE₂, reduce the formation of thromboxane B₂ and regulate DNA and protein synthesis rates in gastric mucosa (Borrelli & Izzo, 2000). In addition, these compounds have a low toxicity and are currently used as therapeutic agents (β -aescin is used for the treatment of peripheral vascular diseases, and GA is a component of herbal drugs used in the therapy of acne, ulcer, and other diseases) (Milgate & Roberts, 1995; Sirtori, 2001).

4.4 FUTURE PERSPECTIVES

The results obtained in this chapter will help to increase our knowledge about the activity of the lipolytic enzymes of *P. acnes* and *H. pylori*, two pathogenic bacteria whose lipase activity is related to the diseases they produce. Knowledge about these lipases, together with a detailed analysis of their enzymatic and gene regulation, could also contribute to better understand how these enzymes function, in order to develop new therapeutic approaches for the treatment of these diseases, including the search and design of new lipase inhibitors. These studies would be of special importance to establish the physiological role and relevance in *H. pylori*-related diseases of EstV. Moreover, it should be also very interesting to determine if this enzyme shows activity on dienoate hydrolase substrates, and to perform a crystallographic analysis of this protein. With respect to *P. acnes* GehA, one of the most attractive challenges would be improving the heterologous expression of this lipase in order to have enough protein level for purification assays. Purified GehA would allow the confirmation of the results obtained for this enzyme, and the crystallographic analysis of this lipase. An improved expression of this protein could be achieved by cloning *gehA* into a more suitable host such as *Bacillus*, which has revealed to be a useful tool for the expression (and secretion) of Gram-positive lipases (Dartois *et al.*, 1994; Sánchez *et al.*, 2002). Another possibility could be to improve the expression of this protein in *E. coli* by adding disaggregating agents, or by inducing the expression of GehA from its own promoter, since *gehA* promoter has shown to function in *E. coli* (Miskin *et al.*, 1997).

Nevertheless, the most promising results obtained in this work correspond to the inhibition by natural substances of both lipases. GA, (\pm)-catechin and kaempferol, being GehA inhibitors, and displaying a wide range of antiacne properties and a low toxicity, are very attractive candidates for the treatment of acne, although further assays are necessary to confirm effectiveness *in vivo* of these compounds in the therapy of acne. Moreover, considering the higher inhibition produced by flavonoids on GehA than on CRL, it would be also very interesting to test the effect on GehA of other flavonoids active on CRL such as 3-hydroxyflavone and 5-hydroxyflavone. Similar considerations can be made with respect to β -aescin and GA, two EstV inhibitors which display a wide range of antiulcer effects and low secondary effects. These saponins could help in the therapy of *H. pylori*-related diseases, although further *in vivo* assays would be necessary to confirm their effectiveness.

5 CONCLUSIONS

- I. *P. acnes* GehA, a lipase previously cloned and overexpressed, and being considered as a major etiological agent in the pathogenesis of acne, has been cloned and characterized in detail.
- II. Analysis of the amino acid sequence of GehA has revealed that this enzyme shows the typical molecular features and structural arrangement of lipases.
- III. GehA displayed an intermediate behaviour between “true” lipases and carboxylesterases, showing maximum activity on medium-chain lipids and also high activity on a wide range of short- and long-chain substrates, and showing no interfacial activation.
- IV. GehA displayed its maximum activity at 37 °C and pH 7 and showed also a high activity from 20 °C to 50 °C and at pH 5–7.5. This enzyme was inhibited by Ag⁺ (at 10 mM), Ba²⁺, Co²⁺, Fe²⁺, Ni²⁺ (at 10 mM), Zn²⁺, NAI, PHMB, EDTA and SDS, whereas Ag⁺ (at 1 mM), Ca²⁺, Hg²⁺, Mg²⁺, Ni²⁺ (at 1 mM) and Pb²⁺ activated GehA. PMSF, urea and the other agents analyzed had no effect.
- V. Analysis of *H. pylori* 26695 genome and proteome revealed that HP0739, a protein putatively annotated as a dienoate hydrolase but showing higher similarity to lipases from family V of bacterial lipases, was the best candidate for producing the lipolytic activity of this pathogen. This protein was named EstV.
- VI. EstV, displaying the typical molecular features and structural arrangements of lipases, has been cloned, purified and characterized.
- VII. EstV displayed the typical behaviour of carboxylesterases, as described for most lipases of family V, showing a marked preference for tributyrin and short-chain *p*-NP- and MUF-derivatives, and displaying a Michaelis-Menten kinetic behaviour with absence of interfacial activation.

- VIII. Maximum activity of EstV was found at 50 °C and pH 10, producing also a high activity from 34 °C to 60 °C and at pH 6–7 and 9–9.5. This enzyme was inhibited by Ag⁺, Co²⁺, Cu²⁺, Fe²⁺, Hg²⁺, Pb²⁺, Zn²⁺, PMSF, EDTA, SDS and urea, whereas Ba²⁺, Ca²⁺ and Mg²⁺ activated EstV. The other agents analyzed had no effect.
- IX. The results obtained for EstV seem to indicate that this enzyme could be the responsible for *H. pylori* carboxylesterase activity detected by Mendz *et al.* (1993), whereas it would not be the main responsible for the lipase activity detected by Slomiany *et al.* (1989a).
- X. We have analyzed the effect on GehA and EstV of the natural substances producing the highest inhibition on *C. rugosa* lipase. In general, these compounds (except glycyrrhizic acid) produced a very different effect on all three lipases, which could be related to the biochemical and structural differences existing among these enzymes.
- XI. GehA was strongly inhibited by (±)-catechin and kaempferol and was moderately inhibited by glycyrrhizic acid and digitonin, whereas the other substances analyzed produced almost no effects on GehA. The inhibition produced by these compounds as well as their other antiacne effects and low toxicity make them promising candidates for the treatment of acne and other *P. acnes*-related diseases.
- XII. EstV was strongly inhibited by reserpine, was moderately inhibited by β-aescin and GA and was activated by (±)-catechin and kaempferol, whereas the other substances analyzed had no effect on the activity of this enzyme. Reserpine has no potential use in ulcer therapy since it is ulcerogenic. On the contrary, β-aescin and GA are very interesting candidates for the therapy of *H. pylori* related-ulcers because a part from inhibiting *H. pylori* EstV, they display a wide range of antiulcer effects and produce a very low toxicity.

6 PUBLICATIONS

The work corresponding to this chapter will be submitted in the following scientific articles (see Annex I):

- **Ruiz, C., Falcocchio, S., Pastor, F.I.J., Saso, L. and Díaz, P.** (2005) *Helicobacter pylori* 26695 ORF HP0739 codes for a previously unknown family V carboxylesterase. Cloning, purification, characterization and inhibition of the enzyme by natural substances. *J. Bacteriol.* Submitted.
- **Falcocchio, S., Ruiz, C., Pastor, F.I.J., Saso, L. and Díaz, P.** *Propionibacterium acnes* GehA lipase: cloning, characterization and inhibition by natural substances. *In preparation.*
- **Ruiz, C., Falcocchio, S., Pastor, F.I.J., Saso, L. and Díaz, P.** Characterization and inhibition of bacterial lipases involved in pathogenesis. *In preparation.*